

A ACTUAL MUDANÇA CLIMÁTICA NO CONTEXTO DA RELAÇÃO ENTRE O CLIMA E AS CIVILIZAÇÕES

FILIPE DUARTE SANTOS

SIM – Laboratório de Sistemas, Instrumentação e Modelação em
Ciências e Tecnologias do Ambiente e do Espaço
Departamento de Física da FCUL

www.sim.ul.pt

1º Encontro Dia Mundial da Meteorologia, IPT
Tomar, 3 de Abril de 2013

Jean-Pierre Perraudin (1767-1858), um guia de montanha e caçador Suíço, foi o primeiro a convencer-se que teria havido mudanças climáticas ao observar os blocos de pedra erráticos e as estrias nas rochas provocadas pelo deslizar das pedras presas ao glaciador, no Vale de Bagnes, Suíça deixados pelo recuo dos glaciares. Convenceu depois o Engenheiro **Ignaz Venetz** que por sua vez deu conhecimento a **Jean de Charpentier** e a **Louis Agassiz** que desenvolveu a teoria do avanço e recuo dos glaciares e das eras glaciais.



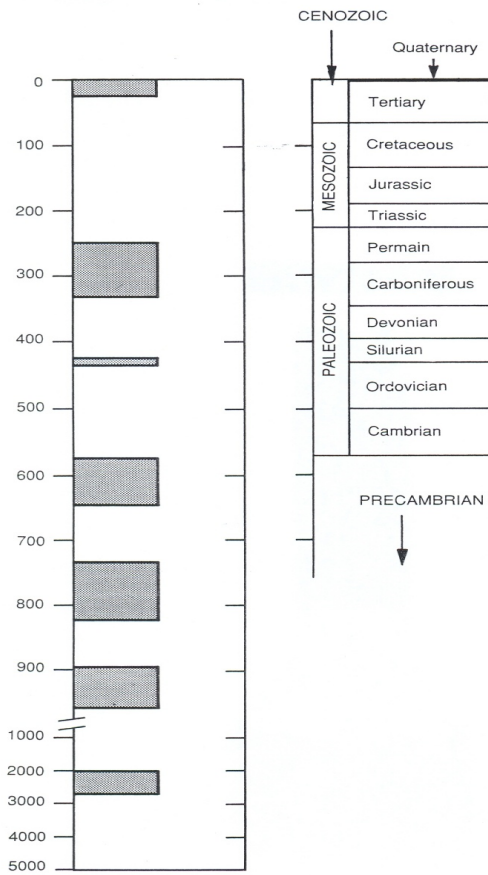
Glacier de Tsanfleuron, Suíça



Striated Graywacke, Yale Glacier, Alaska. 1997

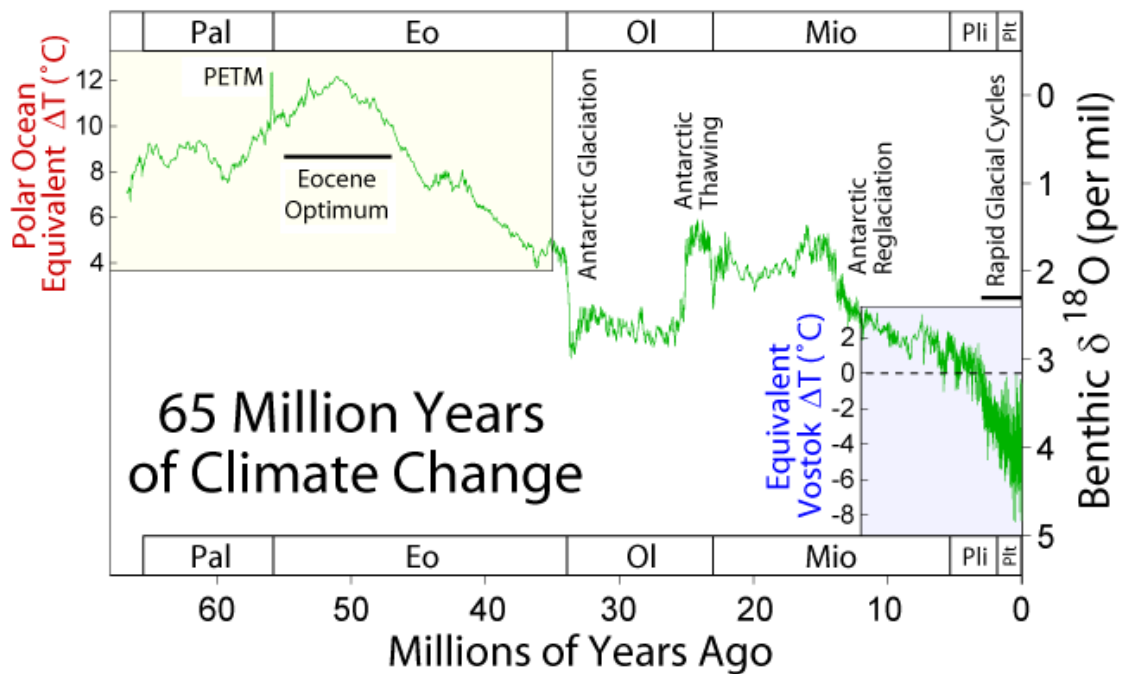


Yosemite National Park, California, USA

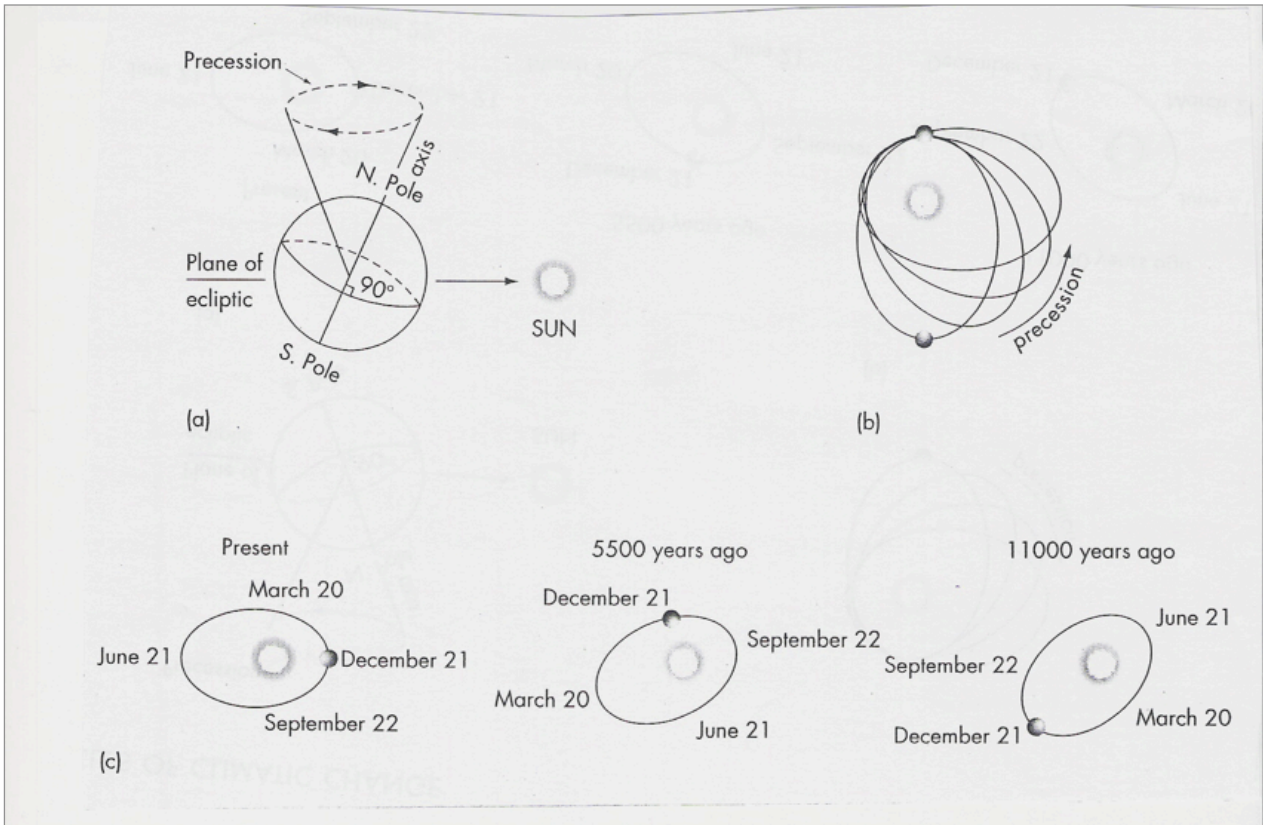


From T.E. Graedel and P.J. Crutzen, 1993

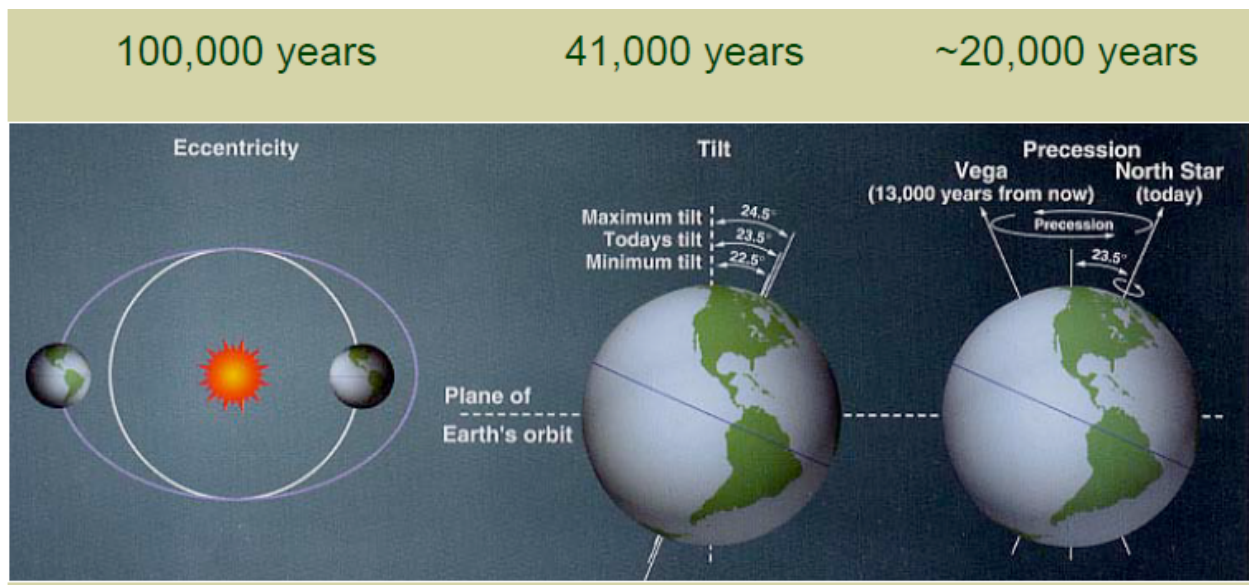
Figure 10.3 Major glacial epochs in Earth's history. Note the change in time scale at 1000 Myr BP. (Reproduced with permission from T. M. L. Wigley, Climate and paleoclimate: What can we learn about solar luminosity variations?, *Solar Physics*, 74, 435-471. Copyright 1981 by Kluwer Academic Publications.)



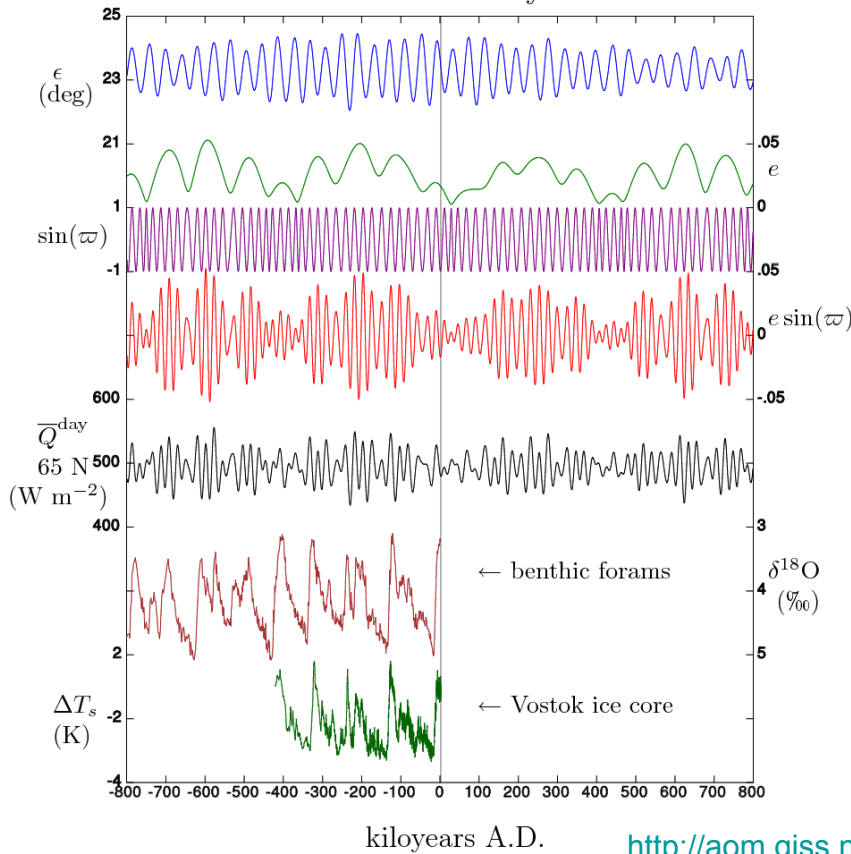
This figure shows climate change over the last 65 million years. The data are based on a compilation of oxygen isotope measurements ($\delta^{18}\text{O}$) on benthic foraminifera by Zachos et al. (2001)



From R.C. Wilson et al., 2000



Milankovitch Cycles



Past and future Milankovitch cycles. [VSOP](#) allows prediction of past and future orbital parameters with great accuracy. ϵ is obliquity (axial tilt). e is eccentricity. ω is longitude of perihelion. $e \sin(\omega)$ is the precession index, which together with obliquity, controls the seasonal cycle of insolation. Q is the calculated daily-averaged insolation at the top of the atmosphere, on the day of the summer solstice at 65 N latitude.

<http://aom.giss.nasa.gov/srorbpar.html>

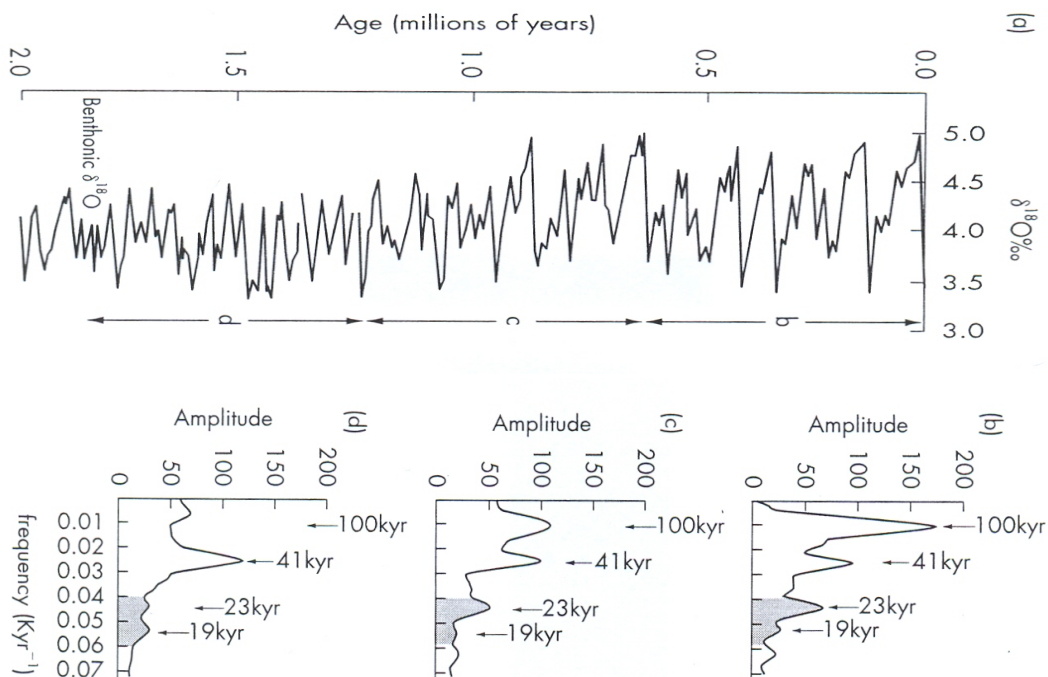
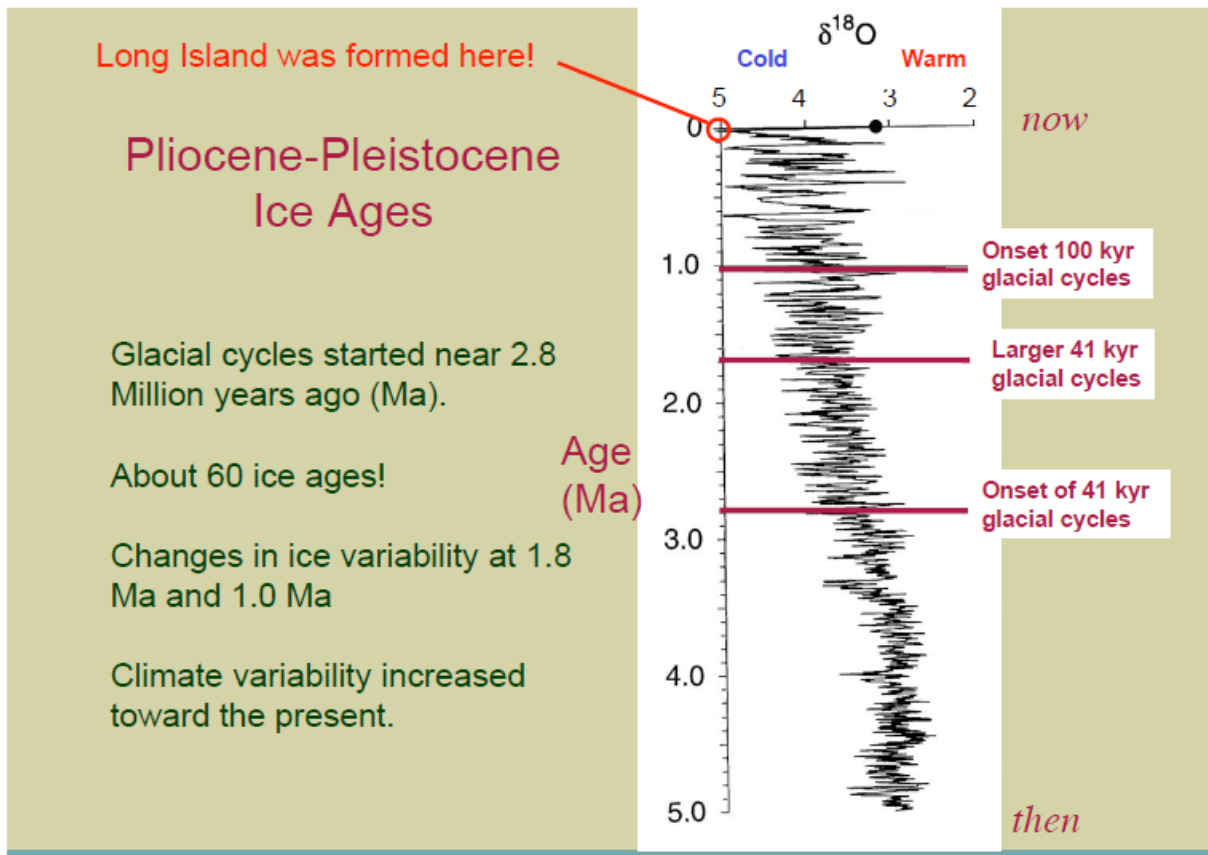
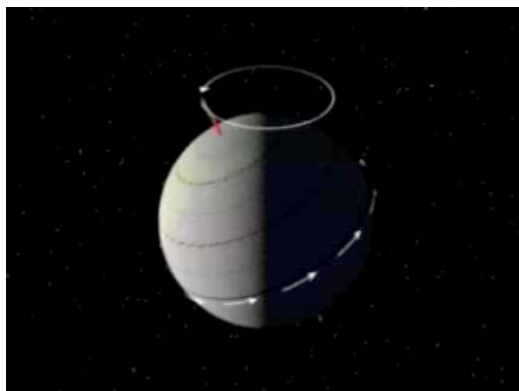


Figure 5.4 Spectral analysis of $\delta^{18}\text{O}$ time series for the past two million years shows that periods characteristic of variations in eccentricity, obliquity and precession are all present in the oceanic record of fluctuations in the volume of land ice.

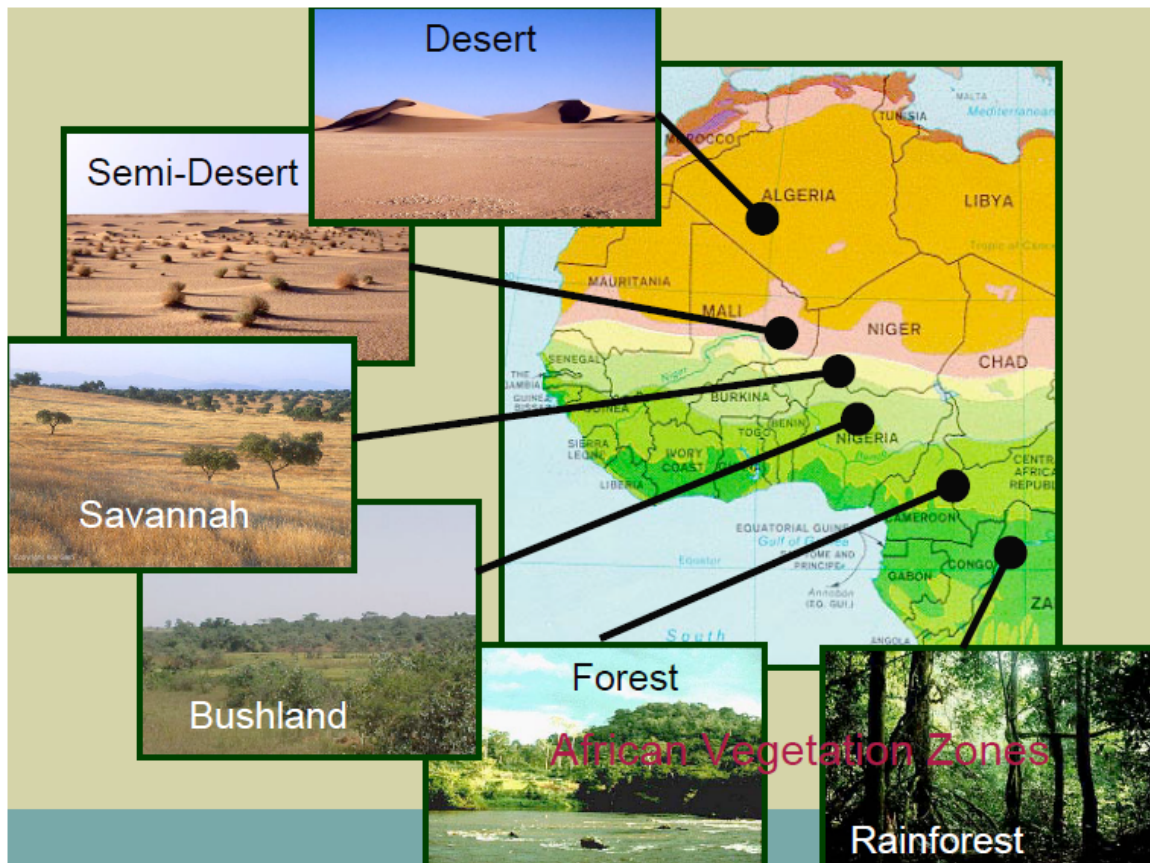
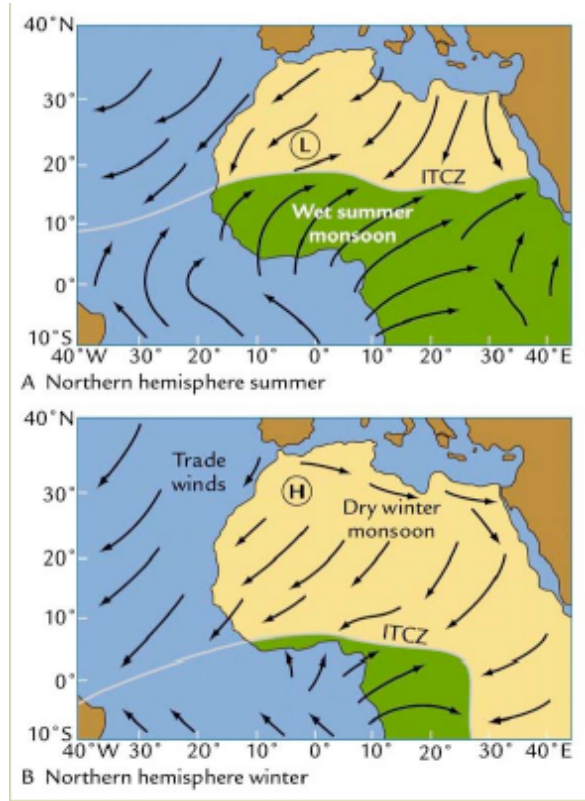
From J. Imbrie et al., 1984



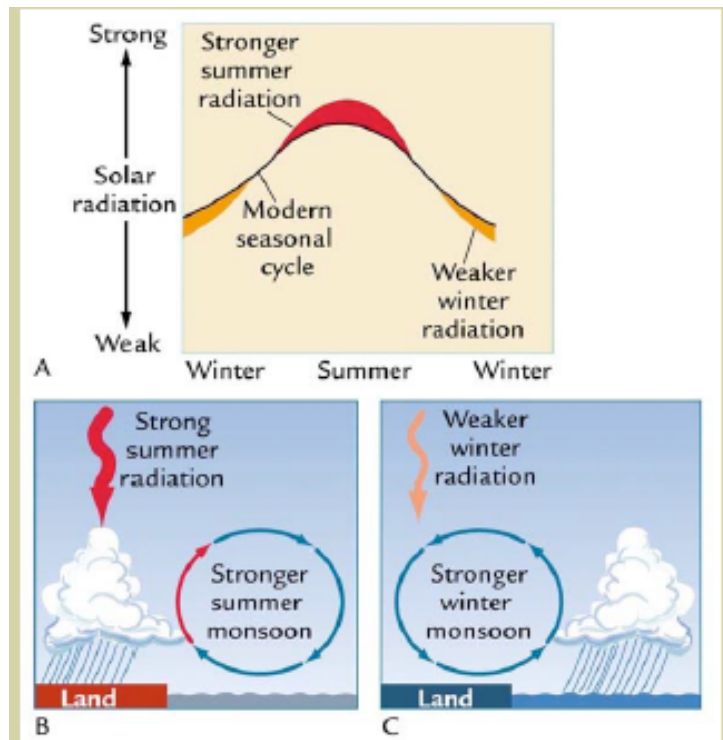
- A precessão, com um ciclo de cerca de 20000 anos, muda a estação do ano em que a Terra está mais próxima do Sol (periélio)
- Consequentemente a precessão afecta a distribuição ou sazonalidade da radiação solar recebida e não a quantidade total anual dessa radiação.
- Quando o periélio se dá no verão boreal a radiação recebida é cerca de 15% superior relativamente ao periélio no inverno boreal



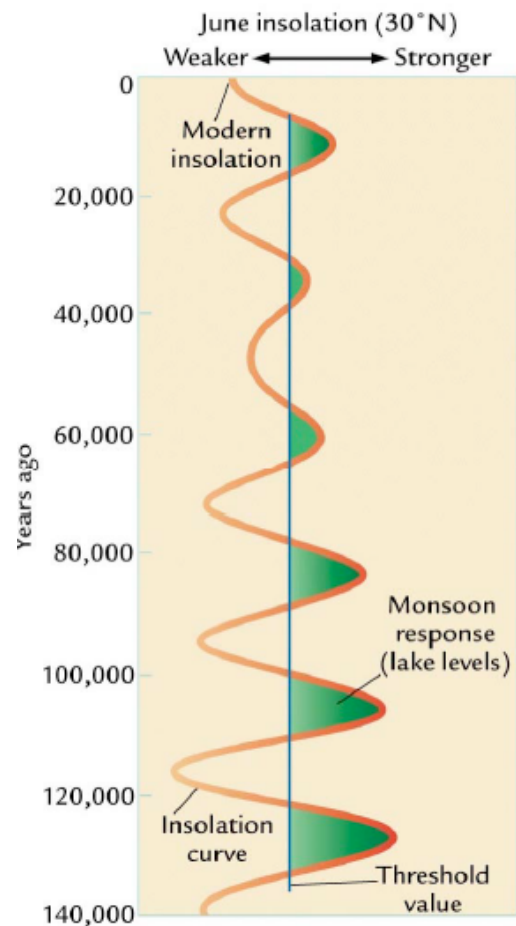
A monção em África caracteriza-se por verões húmidos e invernos secos e determina a distribuição geográfica da vegetação e dos ecossistemas



Quando o movimento de precessão provoca verões boreais mais quentes (tal como, por exemplo, há 9000 anos) a monção estival torna-se mais forte e a África acima do equador mais húmida



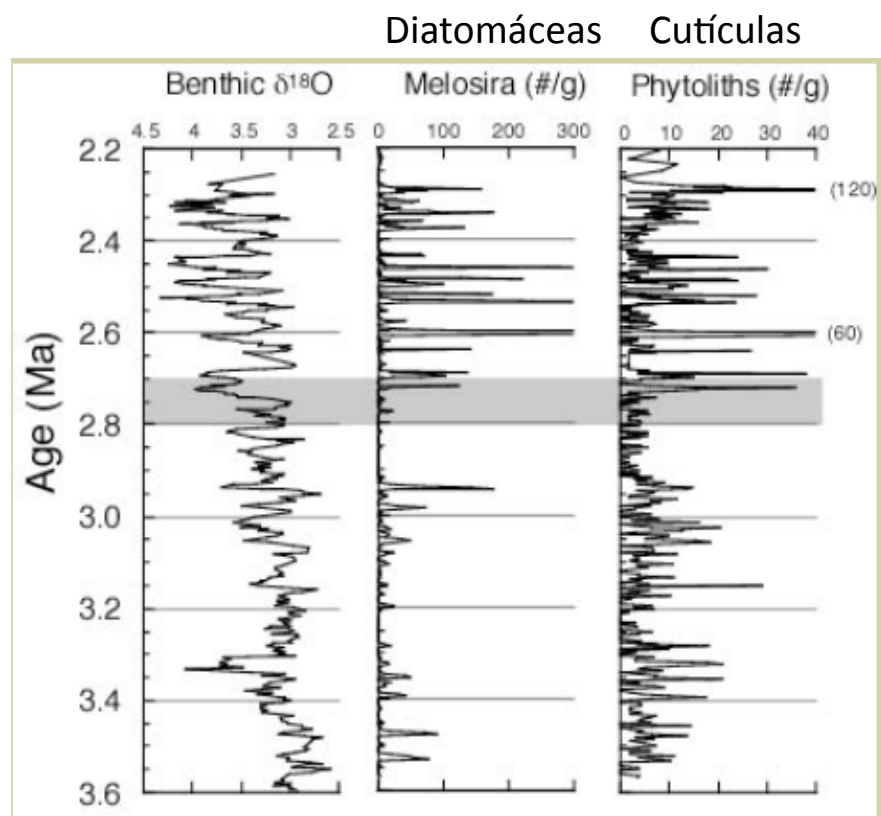
Os períodos húmidos de África ocorreram com uma periodicidade de cerca de 20000 anos, correspondente ao ciclo da precessão



O paleoclima de África reconstrói-se, em parte, com o estudo dos sedimentos depositados no fundo do oceano, através das:

- Concentrações de poeiras transportadas pelo vento (num clima mais seco há mais poeira)
- Diatomáceas de água doce provenientes dos lagos africanos
- Abundancia de cutículas de gramíneas (extensão das pradarias)
- Pólen

O clima africano tornou-se mais seco e variável a partir de 2.8 M.a.



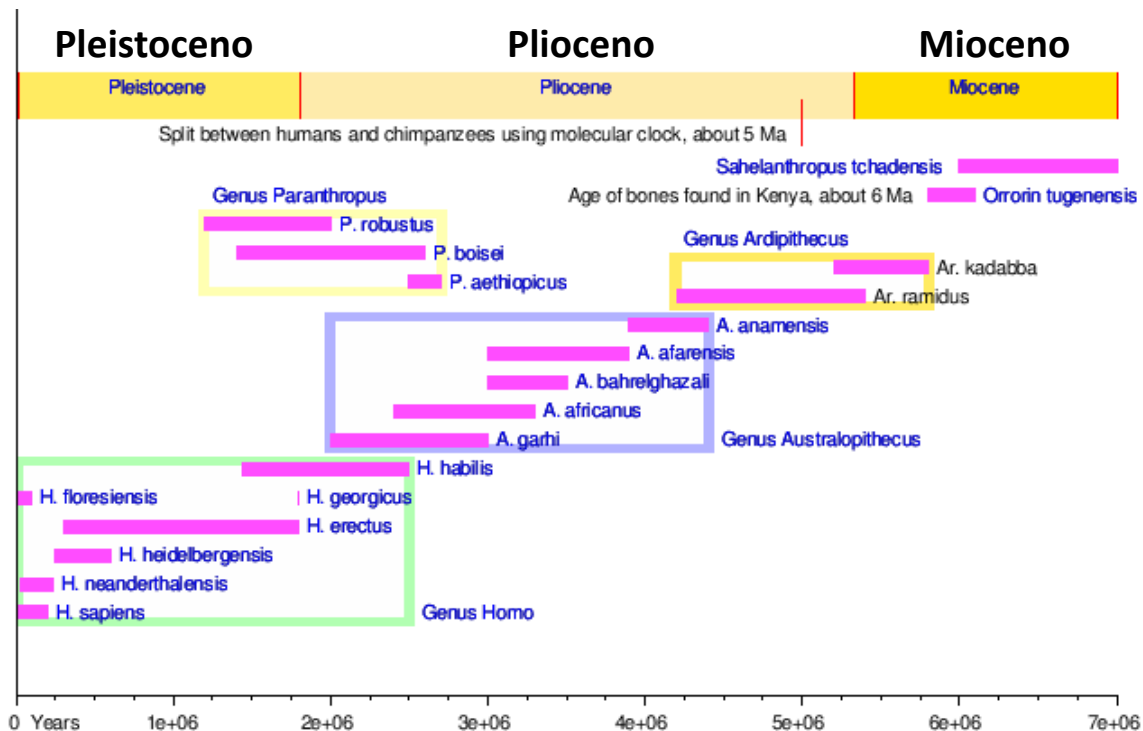
Antes de 2.8 M.a.

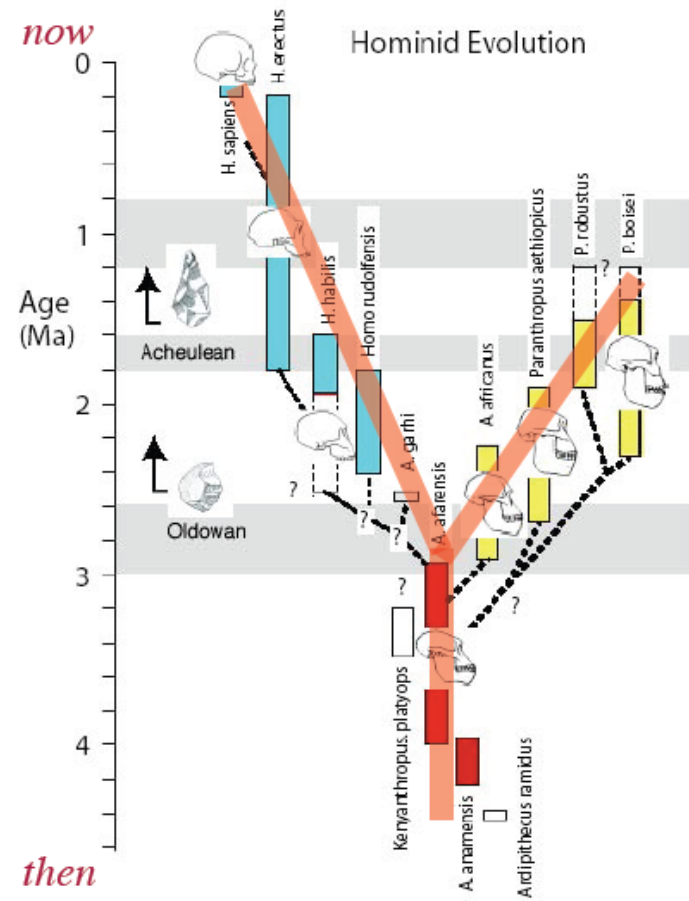
As calotes polares não se tinham ainda formado completamente, especialmente no Ártico, e o clima africano era determinado pelas monções, cuja intensidade é controlada pelo movimento de precessão do eixo da Terra (período de cerca de 20000 anos). Por outras palavras havia apenas um sinal dos ciclos de Milankovitch.

Depois de 2.8 M.a.

A formação da calote polar no Ártico gerou climas mais frios nas latitudes elevadas que conduziram a um clima mais frio, seco e ventoso em África. Passou a haver uma covariação do clima de África com o clima das latitudes elevadas.

Por outras palavras, aos ciclos “húmido-seco” associados ao movimento de precessão adicionaram-se os outros ciclos de Milankovitch, característicos da nova era glacial.

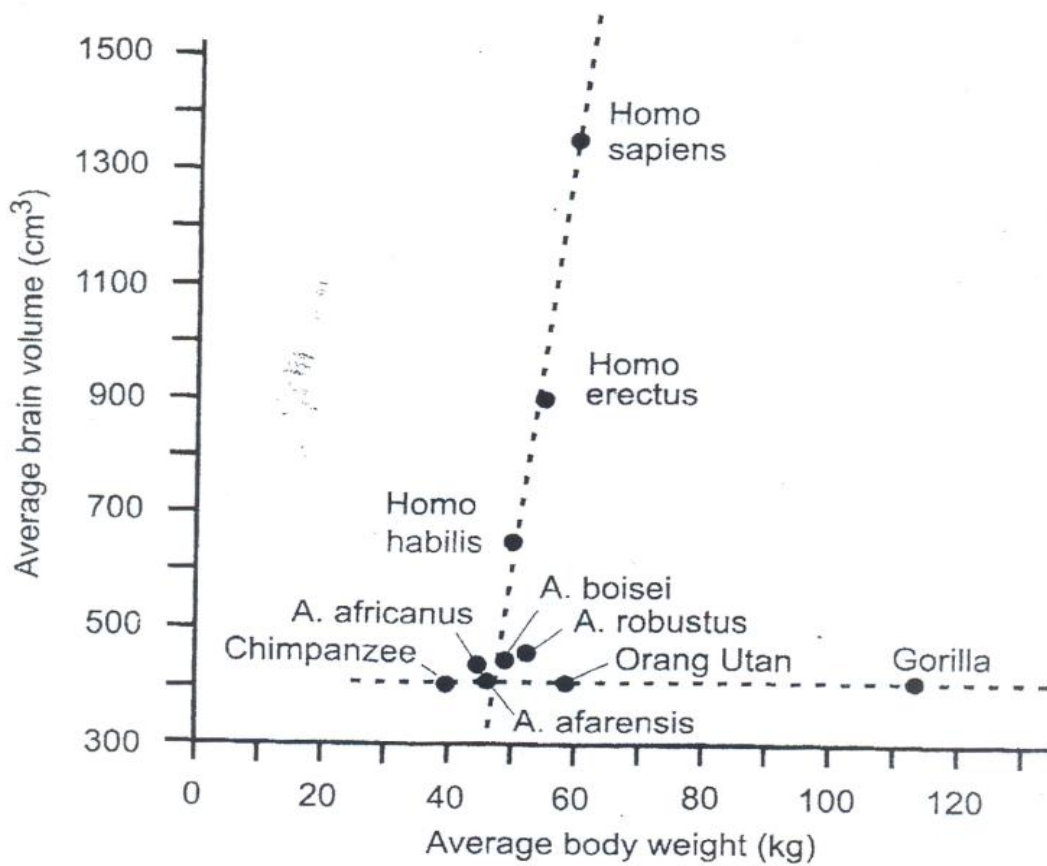
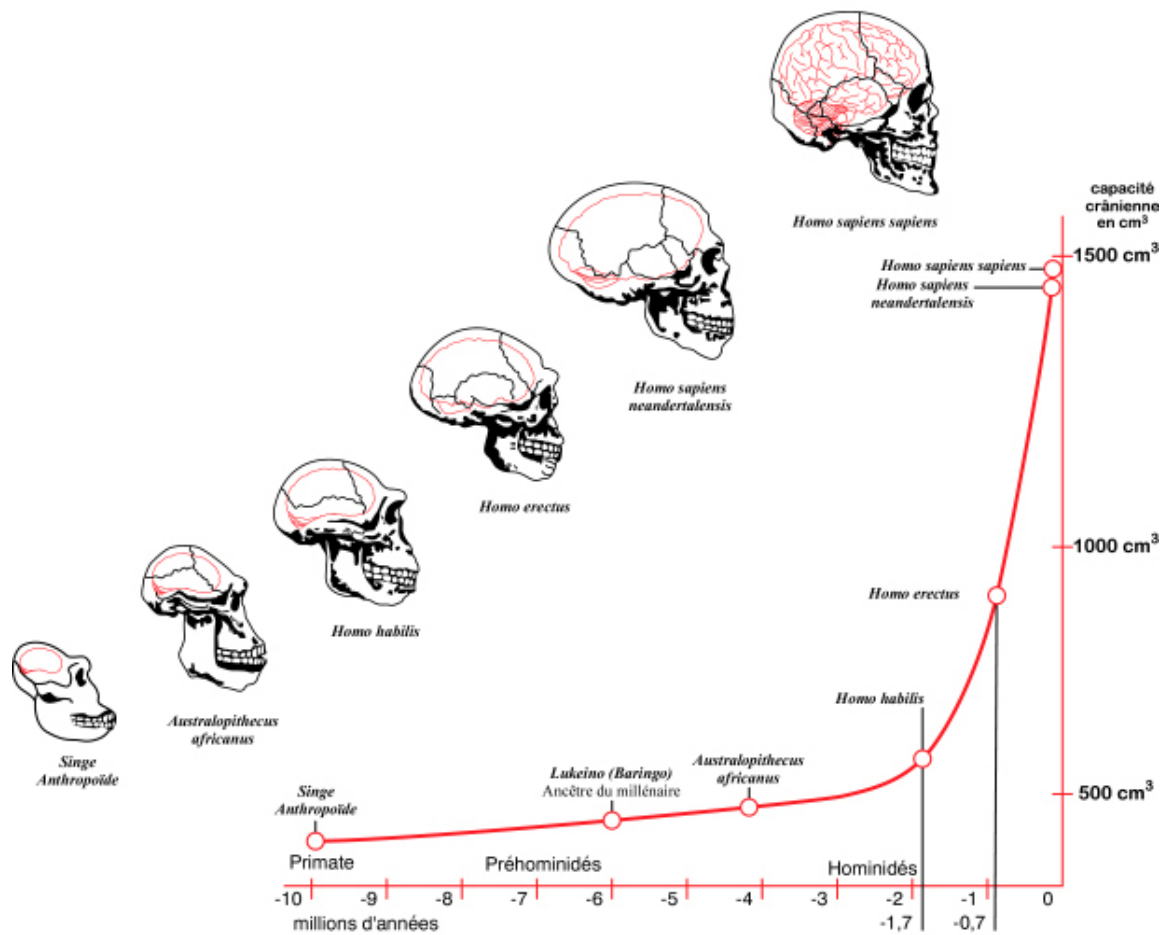




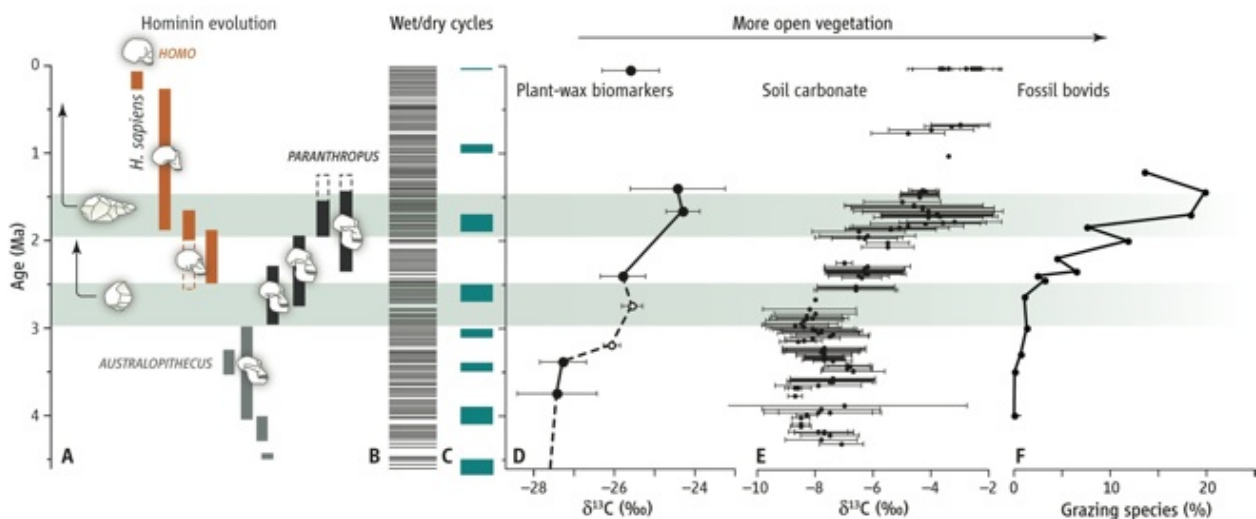
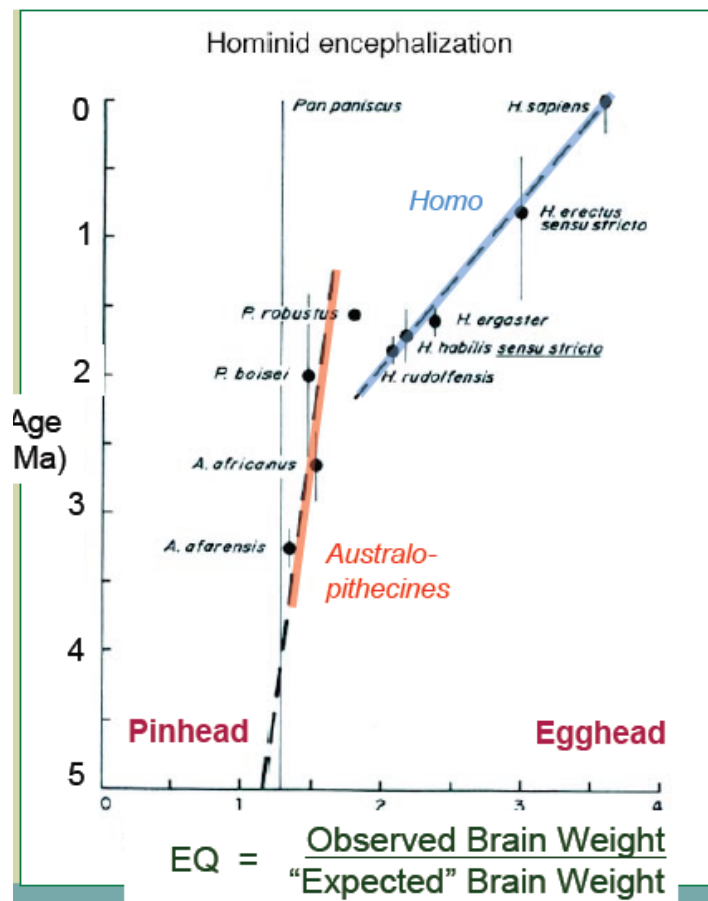
O género Homo surgiu há cerca de 2.6 M.a. e caracteriza-se por um crânio de maior volume (650 cc.), face mais plana, mais alto e grácil, molares de menor dimensão e, provavelmente, primeiros utilizadores de instrumentos líticos. Os mais antigos do Olduvaiense aparecem há cerca de 2.7 M.a.



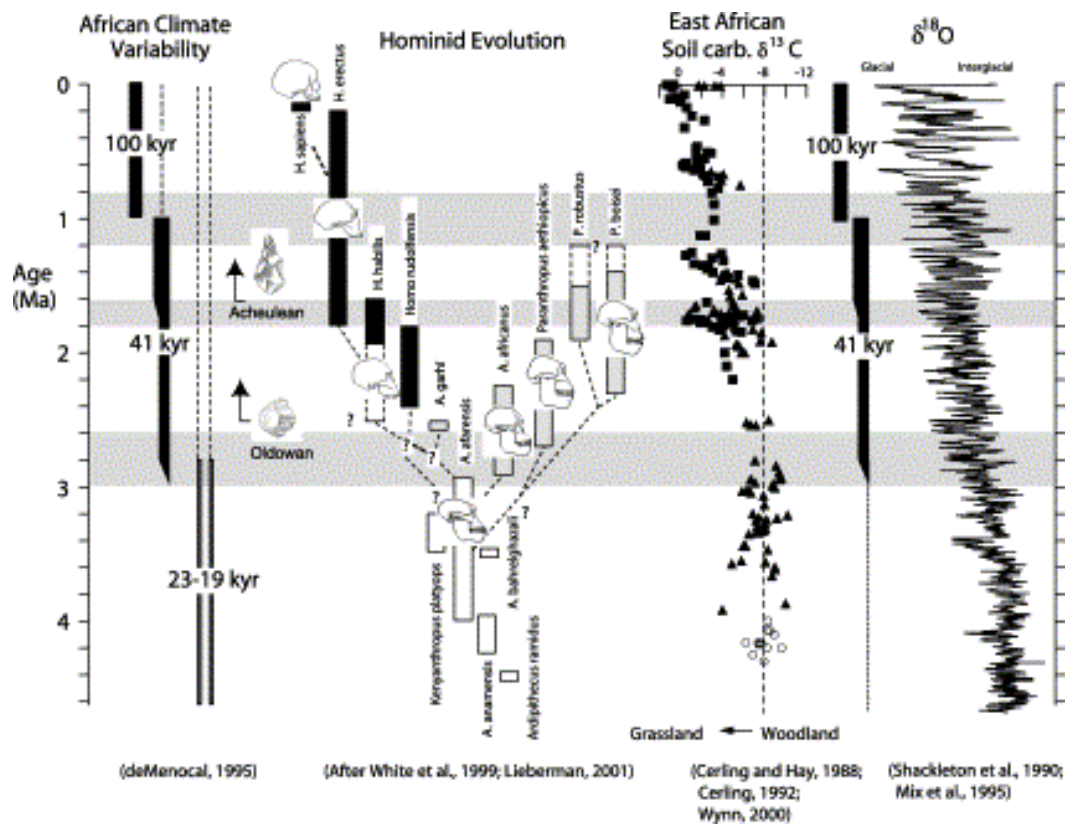
KNM-ER-1813 (Homo habilis)
~1.9 Ma



Coeficiente de encefalização



Above: A snapshot of African evolutionary and paleoclimate changes (Figure from deMenocal, 2011). (A) Summary diagram of human evolution spanning the last 4.6 Ma [no phylogenetic relations are indicated; ranges compiled from the recent NRC Report (2011)]. First appearances and approximate durations of Mode 1 (Oldowan) and Mode 2 (Acheulean) stone tools are indicated (Bobe and Leakey, 2009). (B) Occurrences of Mediterranean sapropel deposits compiled from marine and land sediment sequences (Lourens et al., 1996). (C) Compilation of sedimentary evidence indicating deep lake conditions recorded in several East African paleolake basins (Trauth et al., 2005; Kingston et al., 2007). (D) Carbon isotopic analyses of plant-wax biomarker compounds measured at Site 231 in the Gulf of Aden, currently the most proximal ocean drilling site to hominin fossil localities (Feakins et al., 2005). The shift to higher values after 3 Ma indicates a greater proportions of C₄ vegetation, or savannah grasslands. (data compiled in Wynn et



Peter B deMenocal, Earth and Planet Science Letters, 2004, 220, p. 3-24

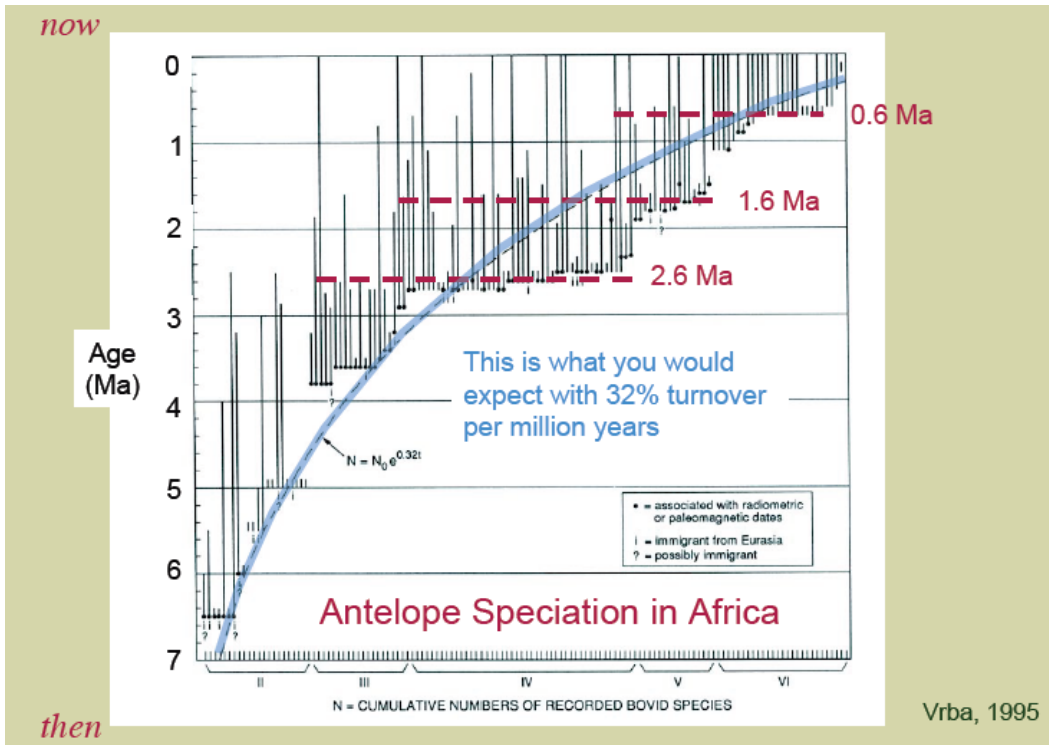
Arid-adapted grazers after 2.8 Ma

- First appearances of many grazer species near 2.8-2.4 Ma
- *Oryx* - one of the most arid-adapted species
- Also, giant Buffalo and Hartebeest.



Oryx

Elizabeth Vrba, 1995



Elizabeth Vrba, 1995

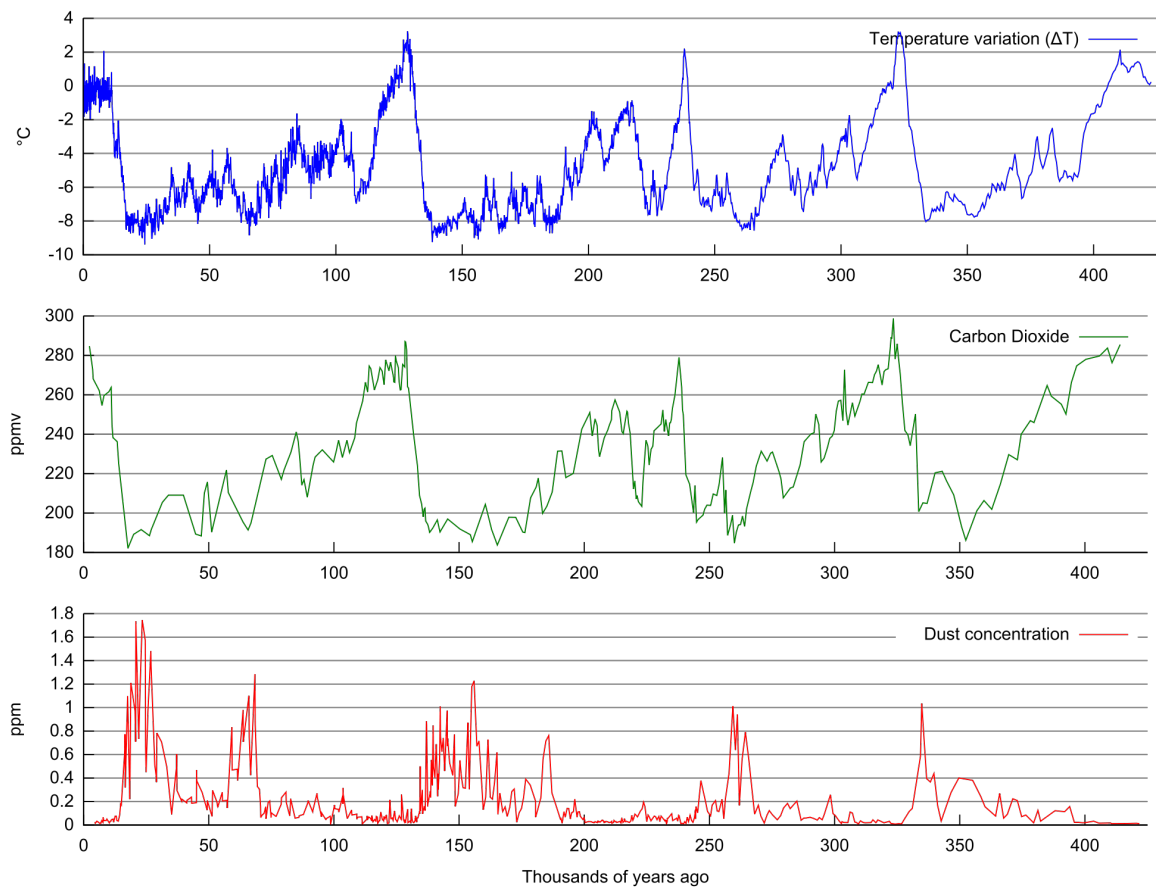


Figure 1 from

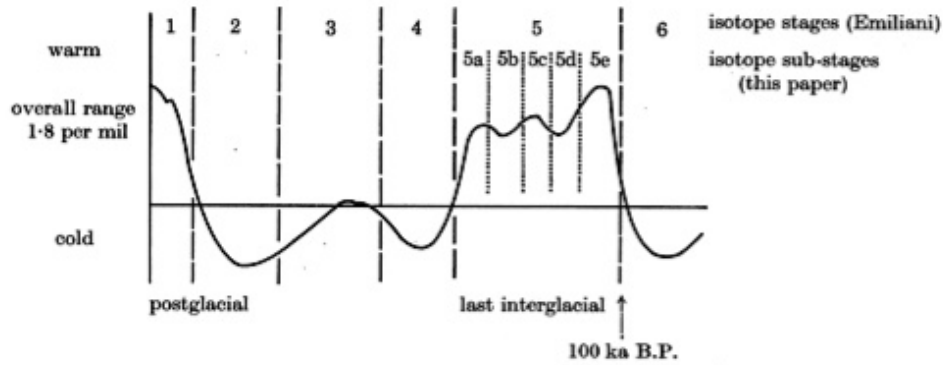


FIGURE 1. Generalized oxygen isotope palaeotemperature record through last six isotope stages, after Emiliani (1961).

MIS 1 - 11 kya, end of the [Younger Dryas](#) marks the start of the [Holocene](#), continuing to the present

MIS 2 - 24 near [Last Glacial Maximum](#)

MIS 3 - 60

MIS 4 - 71 (74)

MIS 5 - 130, includes the [Emian](#); usually sub-divided into a to e:

MIS 5a - 84.74

MIS 5b - 92.84

MIS 5c - 105.92

MIS 5d - 115.105

MIS 5e - 130.115

MIS 6 - 190

MIS 7 - 244

Marine Isotope Stages



O Homem-de-Neandertal e o clima no final do último período glacial

A grande variabilidade climática durante o último período glacial desde há 55000 anos foi provavelmente um dos factores que contribuiu para a extinção do **Homem-de-Neandertal** há aproximadamente 30000 anos

Condições associadas ao último máximo glacial do último período glacial há cerca de 20000 anos e que provavelmente ocorreram também anteriormente



A região limitada a vermelho indica aproximadamente a região ocupada pelo Homem-de-Neandertal nas épocas mais frias do último período glacial

The **Akkadian Empire**, formed in 2300 BC, the world's first, subsumed the independent city states into a single state. It stretched from the Persian Gulf to the Mediterranean and to the headwaters of the Euphrates river in present day Turkey, linking rain fed agricultural fields in northern Mesopotamia with irrigation agriculture in the south.

After about 300 years, the Empire of Akkad suddenly collapsed, almost as fast as it had developed, ushering in a dark age that lasted around 1000 years.

What were the reasons for this collapse? In part, they resulted from man-made environmental degradation, especially desertification.

However, it is likely that there was another cause. **Severe droughts occurred in the middle of the third millennium.**

It was the longest dry spell for 10 000 years, and lasted for about 300 years. **The dry and windy environment probably triggered the collapse of the northern Akkadian provinces, which depended on rain for agriculture (Kerr, 1998).** The combination of anthropogenic environmental changes and natural climate change was very likely the main cause for the decline of the first human empire, a conclusion that may have a highly symbolic connotation.

F.D. Santos, in *Humans on Earth*, Springer, 2011

D.J. Kenneth,
Science, 2012

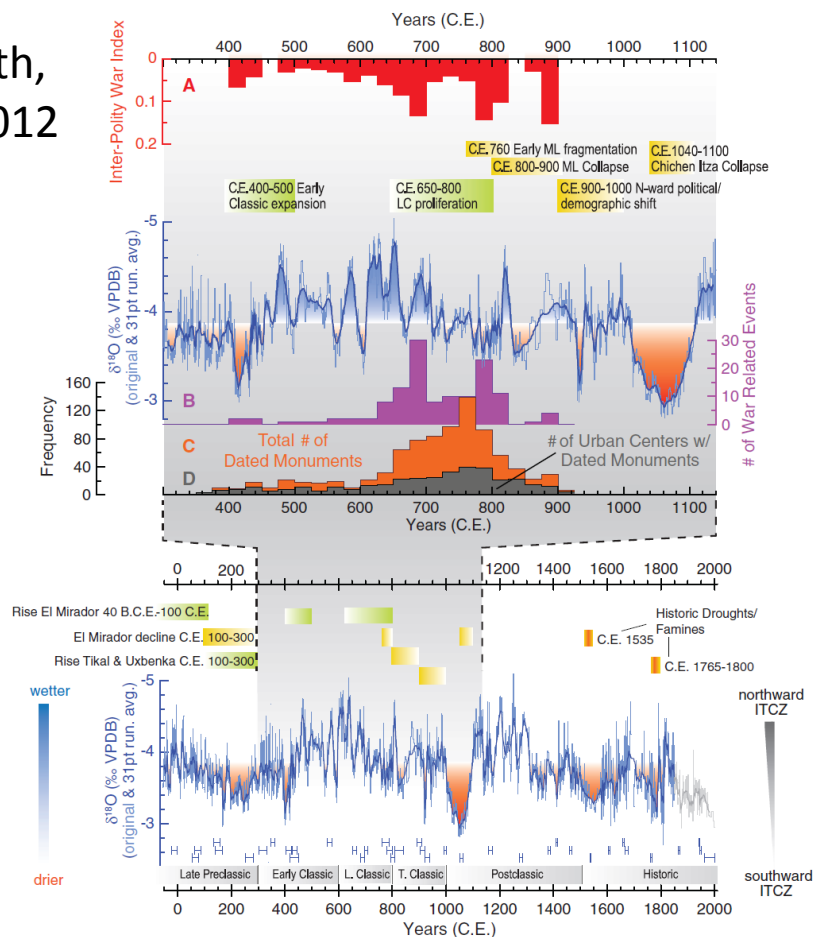
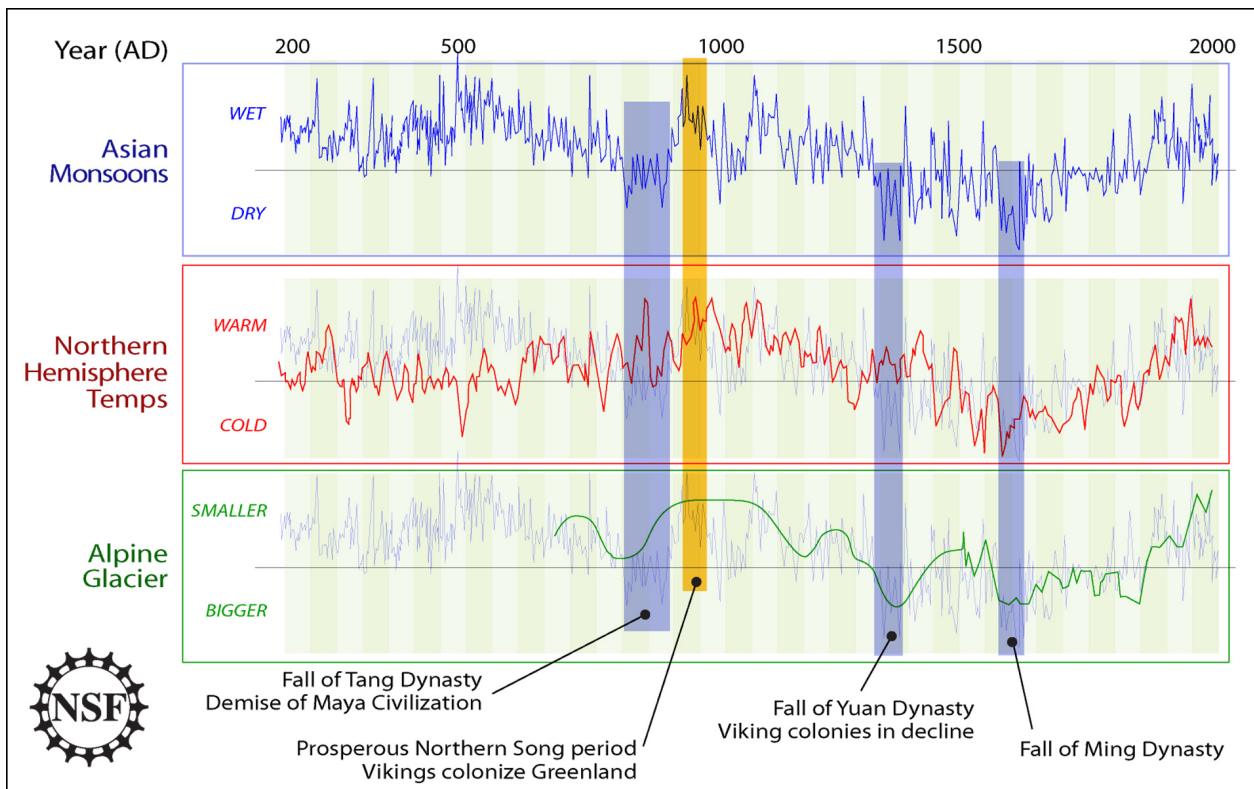
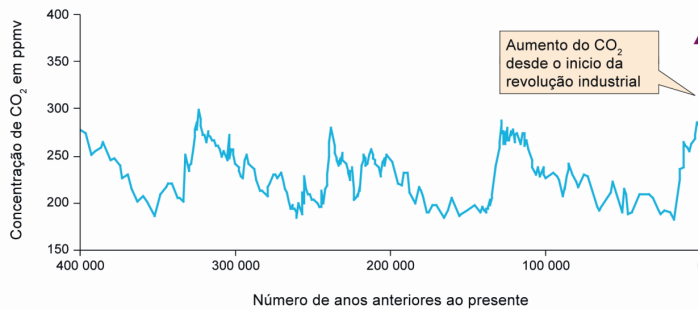
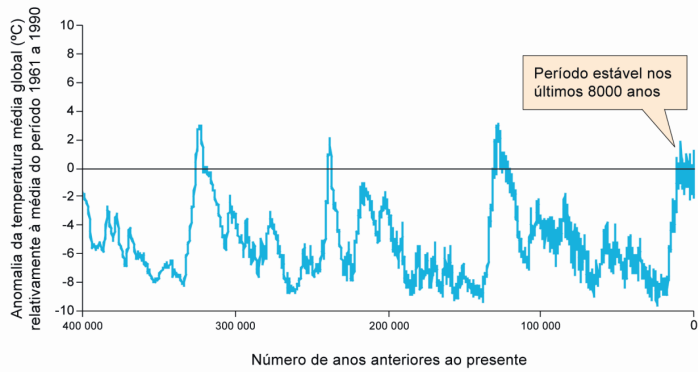


Fig. 2. (Bottom) YOK-I d18O climate record spanning the past 2000 years (40 B.C.E. to 2006 C.E.) shown relative to Maya chronology and major historical events. Blue bars just below the d18O curve indicate the small error for each of the 40 U-Th dates used to constrain the chronology of the d18O climate record (10). Drier-than-average conditions during this interval are shown in orange. Two historically recorded droughts in the 16th- and 18th-century C.E. accord well with the YOK-I record, and the earliest multidecadal drought in the record (200 to 300 C.E.) corresponds with decline of the large center of El Mirador and a major sociopolitical reorganization in the ML. (Top) The YOK-I d18O climate record historic events along with (A) An interpolity warfare index based on the number of war-related events between Maya sites or rulers relative to the total number of events recorded during each interval. (B) Raw number of warrelated events. (C) Frequency distribution of long-count dated monuments in the ML. (D) Total number of urban centers with dated monuments through time as a proxy for the development and disintegration of complex polities in the ML. All hieroglyphic data are from the Maya Hieroglyphic database (raw data is available in the supplementary materials) (28) and are binned in 25-year intervals. The light gray line denotes uncertainties in the 20th century d18O record (10).



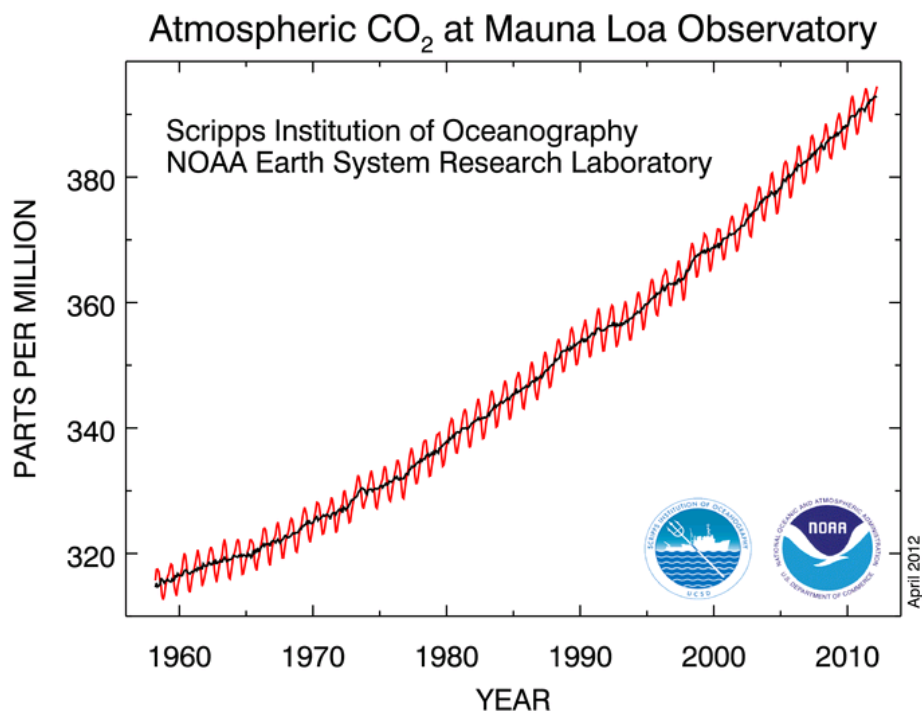
CHINA



Reconstituição da evolução da temperatura média global da baixa atmosfera, representada por meio da anomalia relativamente à média do período de 1961 a 1990, e da concentração atmosférica do CO₂ nos últimos 400 000 anos (Petit, 1999). Figura adaptada de EEA, 2004. Repare-se na correlação que se observa entre os dois registos. O aumento da concentração do CO₂ a partir da revolução industrial e até ao presente está indicado por um vector aproximadamente vertical devido à escala de tempo utilizada na figura

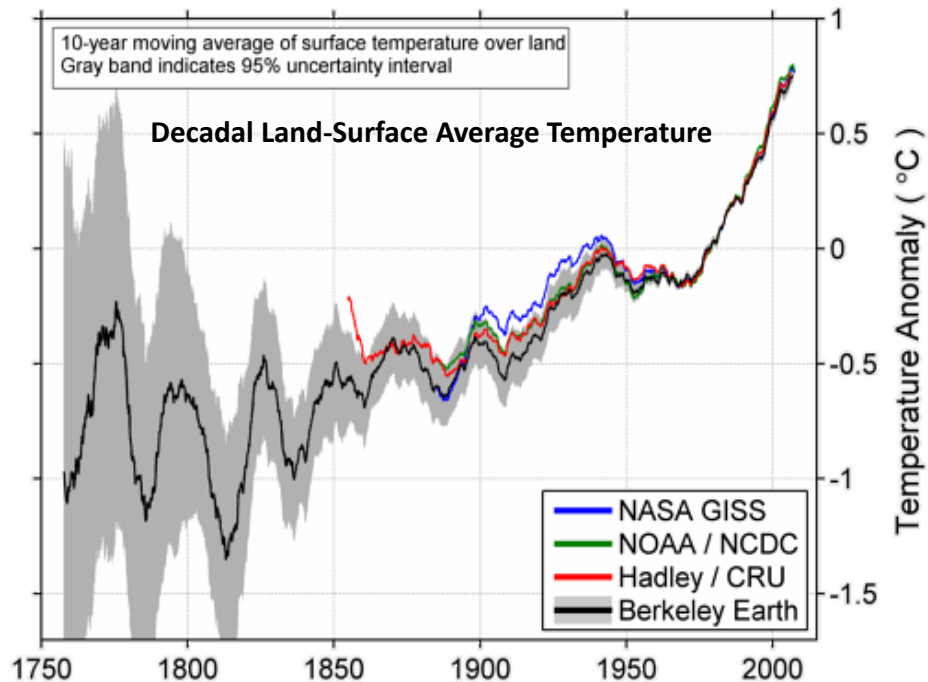
Fonte, Petit et al., 1999

Curva de Keeling de Mauna Loa



Fonte: NOAA, <http://www.esrl.noaa.gov/gmd/obop/mlo/>

Nova Análise da Temperatura Média Global da Atmosfera à Superfície nos Continentes. Uma Confirmação do Aquecimento Global pelos Cépticos (BEST – Berkeley Earth Surface Temperature)



Berkeley Earth, <http://www.berkeleyearth.org>

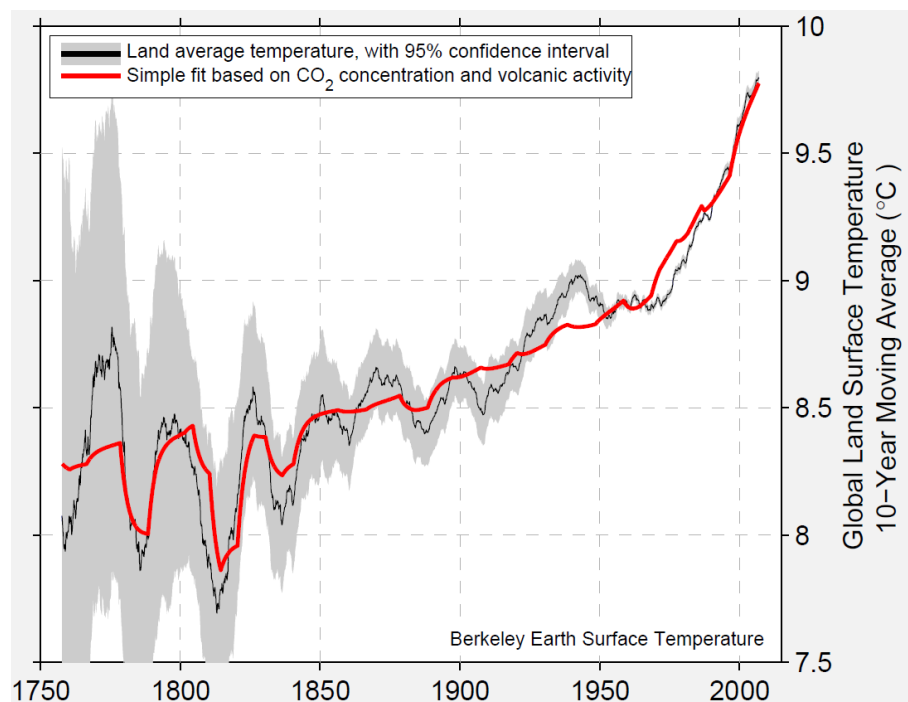
Resultados do Projecto BEST

Linha a vermelho:

Combinação linear de

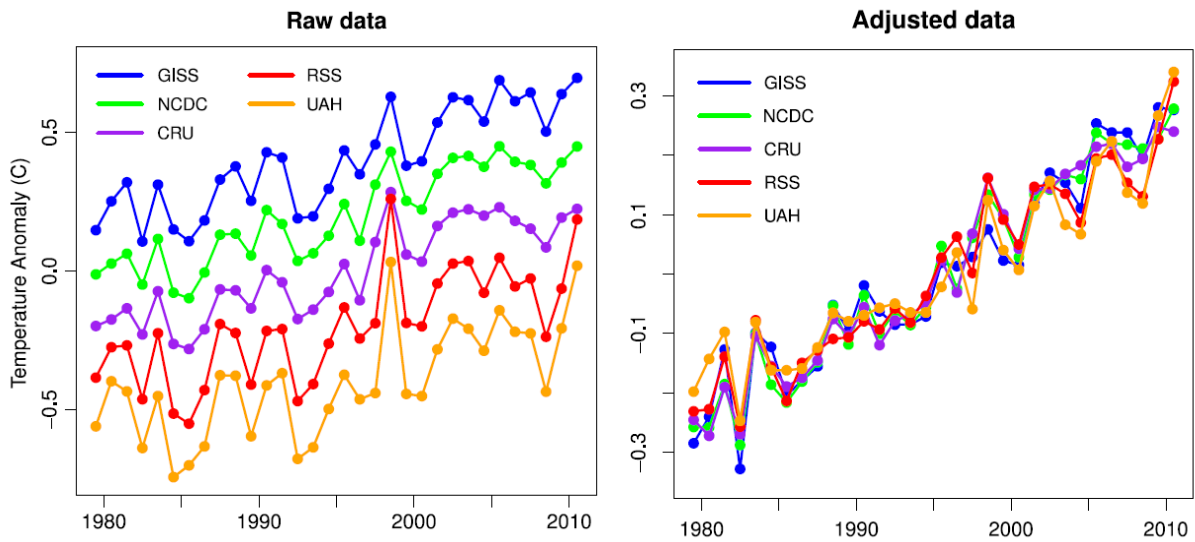
- Emissões vulcânicas de sulfatos
- Logaritmo da concentração atmosférica CO₂.

A inclusão da actividade solar não melhora significativamente o acordo com os dados.



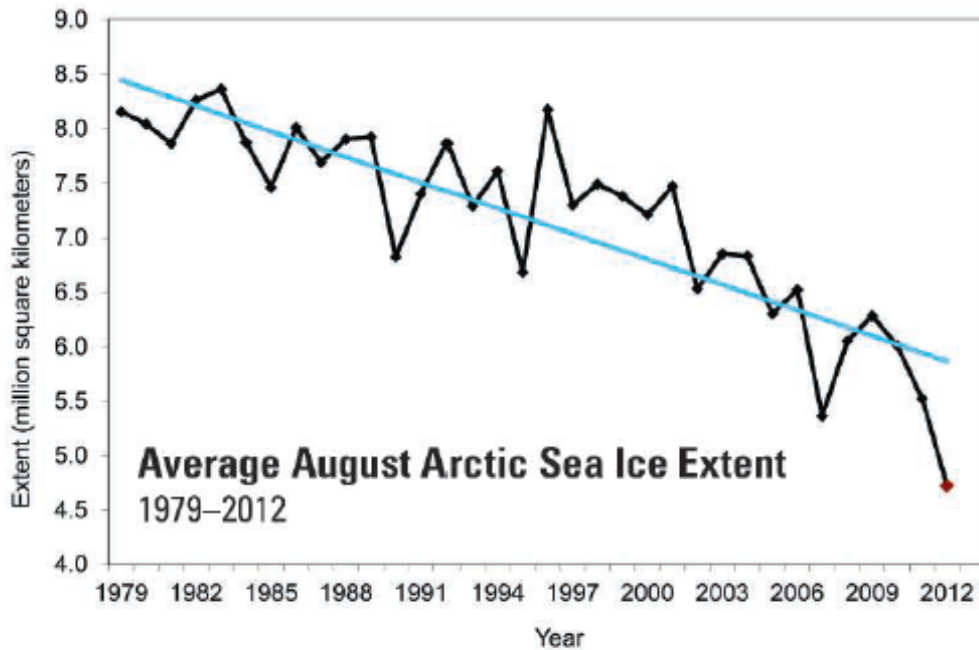
Berkeley Earth Surface Temperature
Berkeley Earth, <http://www.berkeleyearth.org>

Robust Warming Signal over the Last 30 Years



When the data are adjusted to remove the estimated impact of known factors on short-term temperature variations (El Niño/southern oscillation, volcanic aerosols and solar variability), the global warming signal becomes even more evident as noise is reduced.“

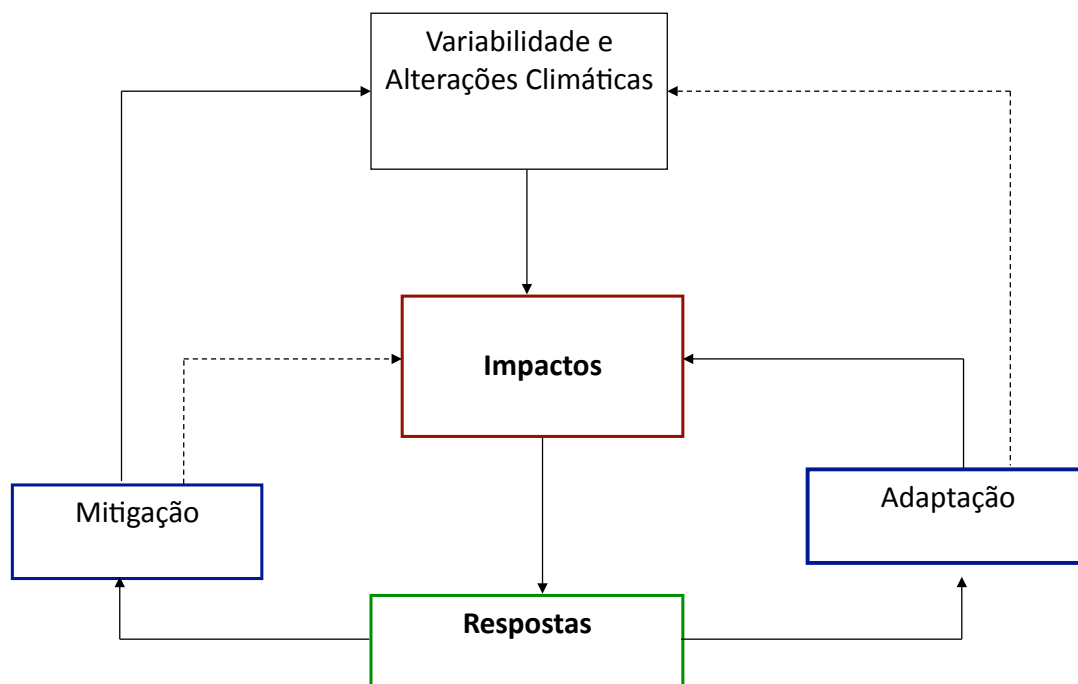
(Foster & Rahmstorf 2011, ERL)



No stopping now. The area of Arctic summer sea ice has been declining rapidly since satellite observations began.

Source: R.A. Kerr, Science, 2012, 337, 1591, 28 September 2012

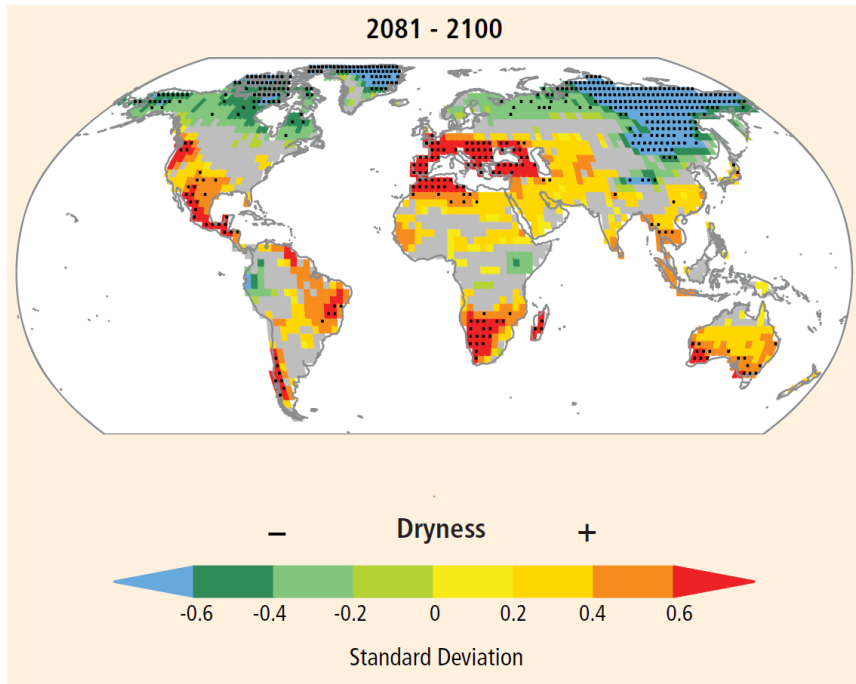
WORLD BANK, 2012		Confidence in attribution to climate change	Impact, costs
Region (Year)	Meteorological Record-breaking Event		
England and Wales (2000)	Wettest autumn on record since 1766. Several short-term rainfall records ²	Medium based on ³⁻⁵	~£1.3 billion ³
Europe (2003)	hottest summer in at least 500 years ⁶	High based on ^{7,8}	Death toll exceeding 70,000 ⁹
England and Wales (2007)	May to July wettest since records began in 1766 ¹⁰	Medium based on ^{3,4}	Major flooding causing ~£3 billion damage ¹¹
Southern Europe (2007)	Hottest summer on record in Greece since 1891 ¹¹	Medium based on ^{8,12-14}	Devastating wildfires
Eastern Mediterranean, Middle-East (2008)	Driest winter since 1902 (see Fig. 20)	High based on ¹⁵	Substantial damage to cereal production
Victoria (Aus) (2009)	Heat wave, many station temperature records (32–154 years of data) ¹⁷	Medium based on ^{8,14}	Worst bushfires on record, 173 deaths, 100,000 houses destroyed ¹⁷
Western Russia (2010)	Hottest summer since 1500 ¹⁸	Medium based on ^{8,13,14,19}	500 wildfires around Moscow, crop failure of ~25%, death toll ~55,000, ~US\$150 billion economic losses ¹⁸
Pakistan (2010)	Rainfall records ²⁰	Low to Medium based on ^{21,22}	Worst flooding in its history, nearly 3000 deaths, affected 20M people ²³ .
Colombia (2010)	Heaviest rains since records started in 1969 ²⁶	Low to Medium based on ²¹	47 deaths, 80 missing ²⁶
Western Amazon (2010)	Drought, record low water level in Rio Negro ²⁷	Low ²⁷	Area with significantly increased tree mortality spanning 3.2 million km ² ²⁷
Western Europe (2011)	Hottest and driest spring on record in France since 1880 ²⁸	Medium based on ^{8,14,29}	French grain harvest down by 12%
4 US states (TX, OK, NM, LA) (2011)	Record-breaking summer heat and drought since 1880 ^{30,31}	High based on ^{13,14,31,32}	Wildfires burning 3 million acres (preliminary impact of \$6 to \$8 billion) ³³
Continental U.S. (2012)	July warmest month on record since 1895 ³⁴ and severe drought conditions	Medium based on ^{13,14,32}	Abrupt global food price increase due to losses ³⁵



————— Efeitos directos ou retroacção

----- Efeitos indirectos

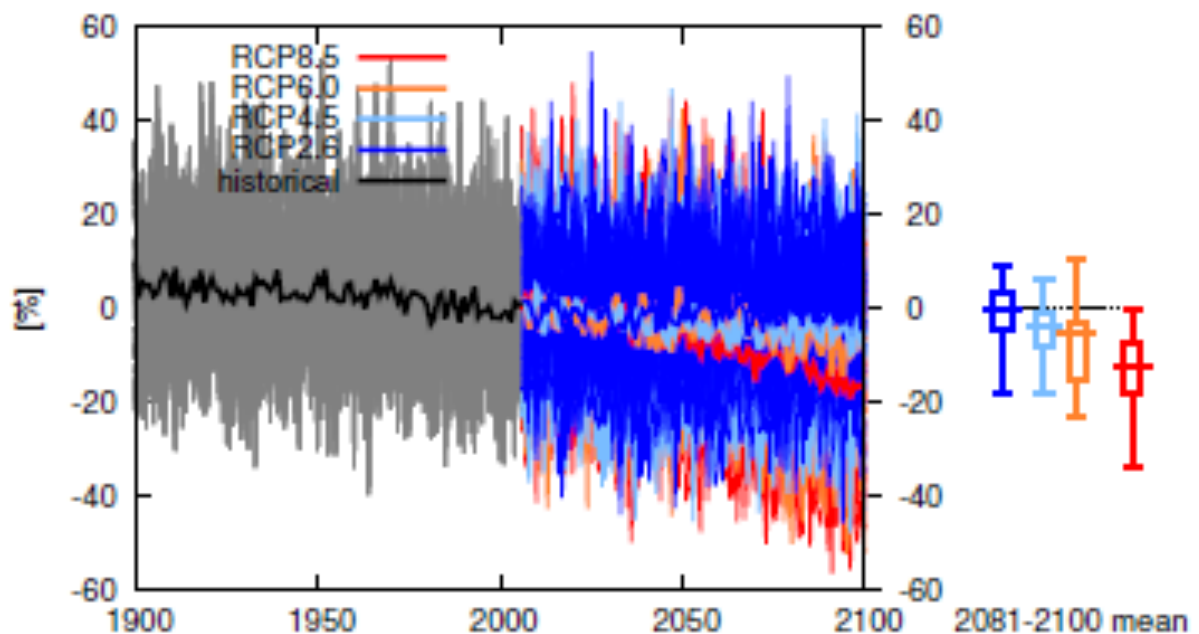
Decrescimento da Precipitação nas Regiões Áridas



Fonte: SREX, IPCC 2012

Varição no número máximo anual de dias consecutivos secos (CDD: Dias com precipitação inferior a 1 mm). Projecções da variação para o final do século, comparativamente ao final do século XX, com GCMs, utilizando o cenário SRES A2.

Precipitation in Southern Europe/ Mediterranean Region, IPCC WGI



Climate scenarios based on Representative Concentration Pathways (RCP)

How Many Gigatons of Carbon Dioxide...?

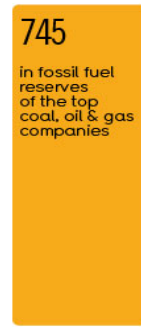
have we released to date?



more can we "safely" release*?



are left to release?



CURRENT HUMAN EMISSIONS PER YEAR **31** gigatons

* before 2050 and still have a chance of staying below 2°C warming

TIME BEFORE WE BREAK OUR 'CARBON BUDGET'



13 YEARS
average yearly emissions increase: 3%

	0.8°C	1.5°C	2°C	3-4°C	5-6°C	
GLOBAL WARMING IF RELEASED	+0.8°C 1.4°F	+1.5°C 2.7°F	+2°C 3.6°F	+3-4°C 5.4-7.2°F	+5-6°C 9-10.8°F	over pre-industrial average temperature
SCENARIO	happened	inevitable	"safe" limit	tipping point	nightmare	
SEA LEVEL RISE BY 2100		0.85m	1.04m	1.24m	1.43m	relative to 1990 sea level
DROWNING CITIES						knee-high flooding

Annual regional carbon dioxide emissions from fuel combustion between 1971-2009

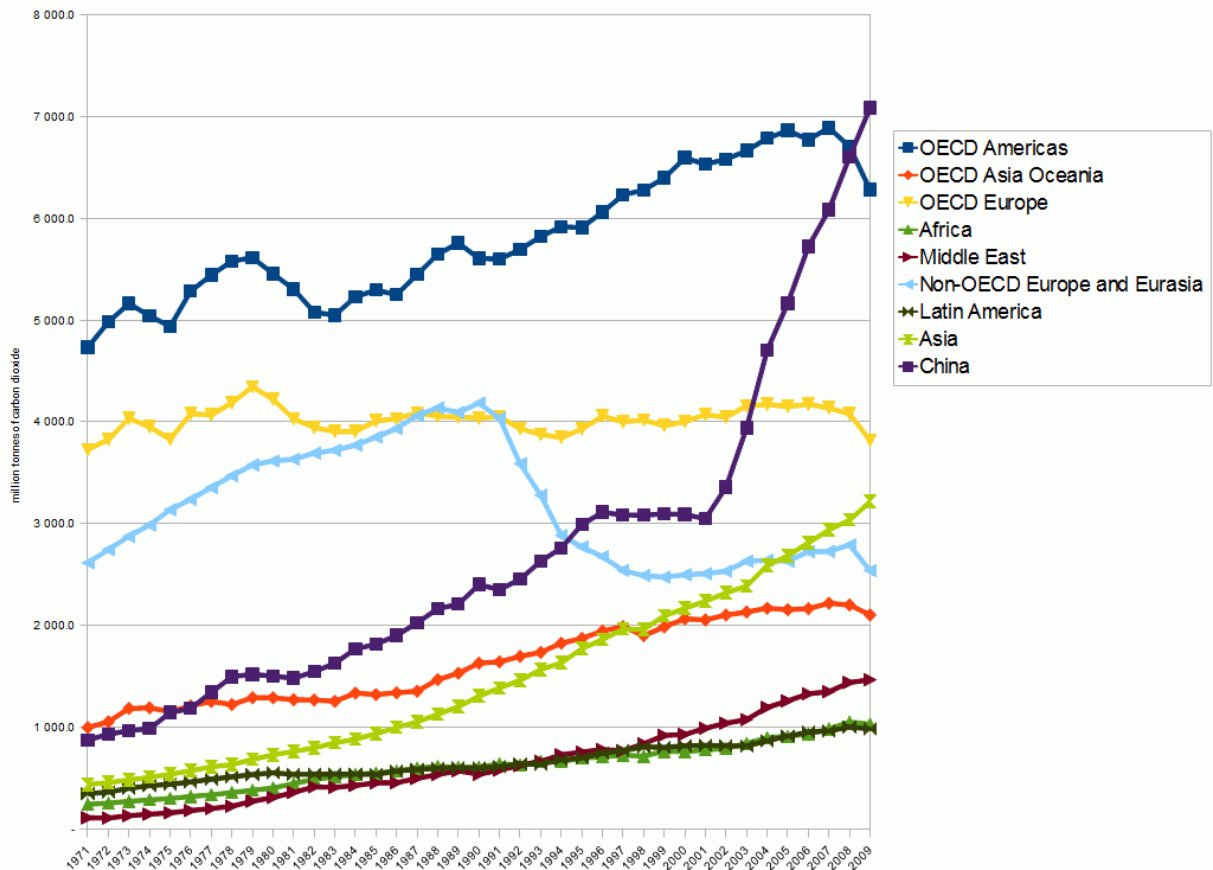


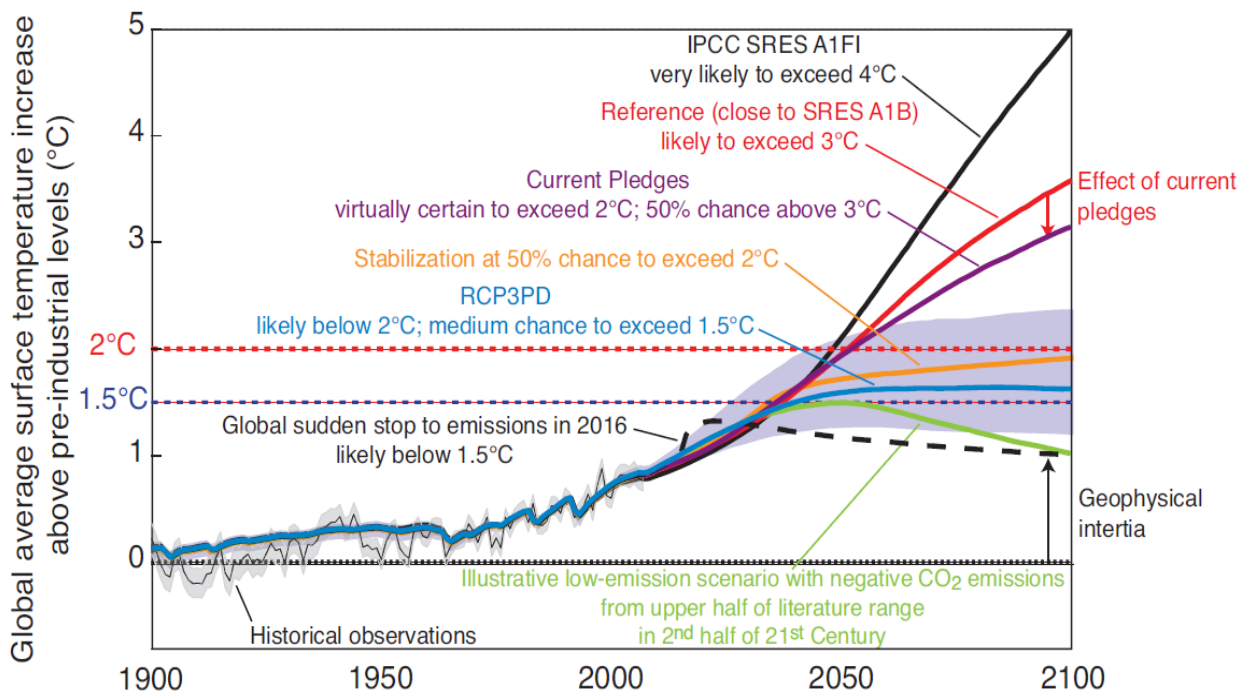
Table 4.1-3

Potential emissions as a consequence of the use of fossil reserves and resources. Also illustrated is their potential for endangering the 2°C guard rail. This risk is expressed as the factor by which, assuming complete exhaustion of the respective reserves and resources, the resultant CO₂ emissions would exceed the 750 Gt CO₂ budget permissible from fossil sources until 2050 (Box 1.1-1). The figures refer to CO₂ alone, other greenhouse gases have not been taken into account. They are based on the values in Table 4.1-2.

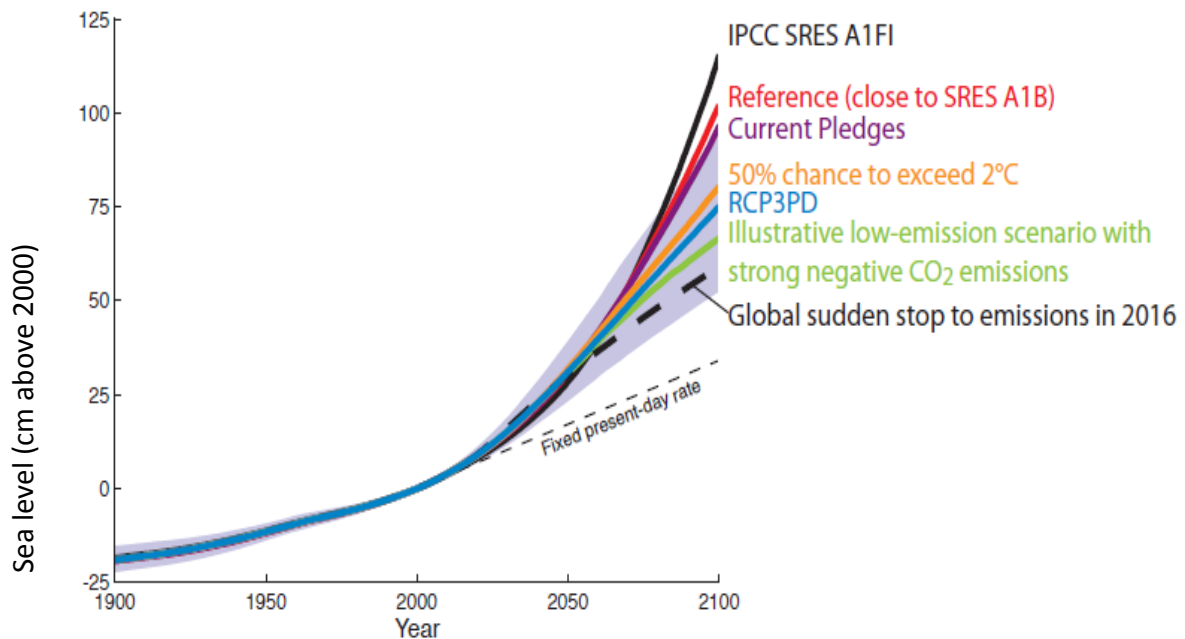
Source: based on Table 4.1-1 and GEA, 2011

	Historical production up to 2008	Production in 2008	Reserves	Resources	Further occurrences	Total: reserves, resources and further occurrences	Factor by which these emissions alone exceed the 2°C emissions budget
	[Gt CO ₂]	[Gt CO ₂]	[Gt CO ₂]	[Gt CO ₂]	[Gt CO ₂]	[Gt CO ₂]	
Conventional oil	505	13	494	386	–	880	1
Unconventional oil	39	2	295	2,637	3,646	6,577	9
Conventional gas	194	7	343	459	27,977	28,778	38
Unconventional gas	15	1	3,987	5,300	–	9,287	12
Coal	666	14	1,970	41,277	–	43,247	58
Total fossil fuels	1,419	37	7,088	50,060	31,622	88,770	118

Efeito dos Actuais Compromissos de redução das Emissões



Global Mean Sea Level: A Semi-Empirical Approach



FP7 EU PROJECT at SIM – CCIAM Research Center

BASE - Bottom-up Climate Adaptation Strategies towards a Sustainable Europe

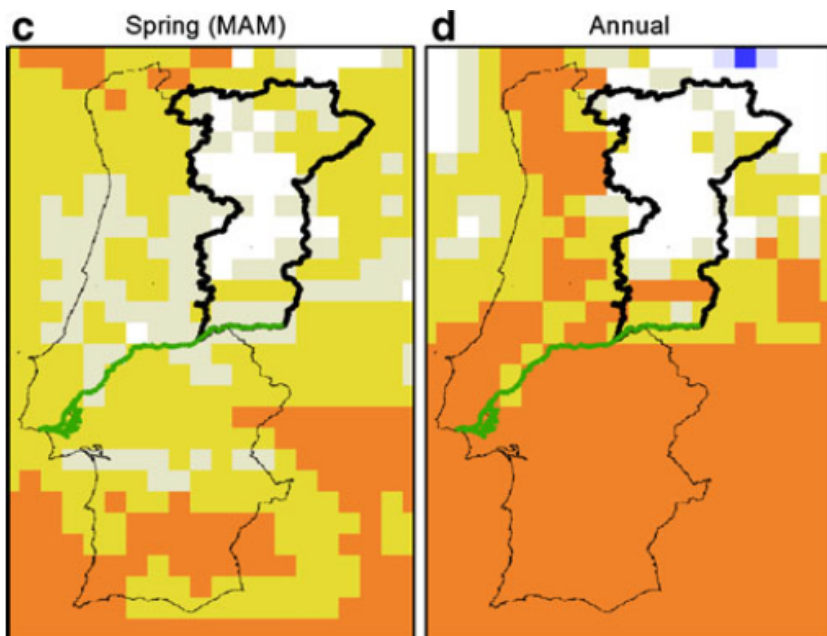
Start date: November 2012 | End Date: 2015

FP7 Env.2012.6.1-3 Total grant: 5.900.000 €

The Bottom-up Climate Adaptation Strategies towards a Sustainable Europe (BASE) project will address the need for research on sustainable climate adaptation strategies, which promote interactions between bottom-up and top-down assessments. The intention is to evaluate the environmental, social and economic impacts, the costs and benefits, policy coherence and stakeholder perceptions of different climate adaptation pathways from an interdisciplinary perspective. The findings from BASE will feed into the European Clearing House Mechanism (CHM) portal and adaptation support tools for policy development.

From the CCIAM Research Group

OBRIGADO PELA VOSSA ATENÇÃO



□ Median in 2071/2100 < Median in 1961/2000, but not significant

□ significant at the 90% conf. level

□ significant at the 95% conf. level

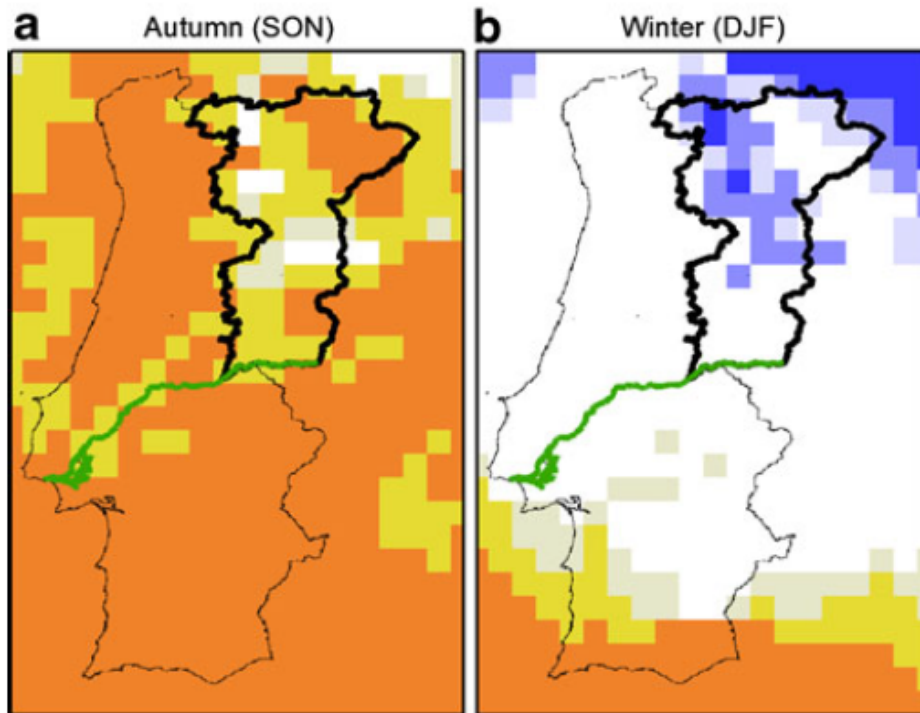
□ significant at the 99% conf. level

□ Median in 2071/2100 > Median in 1961/2000, but not significant

□ significant at the 90% conf. level

□ significant at the 95% conf. level

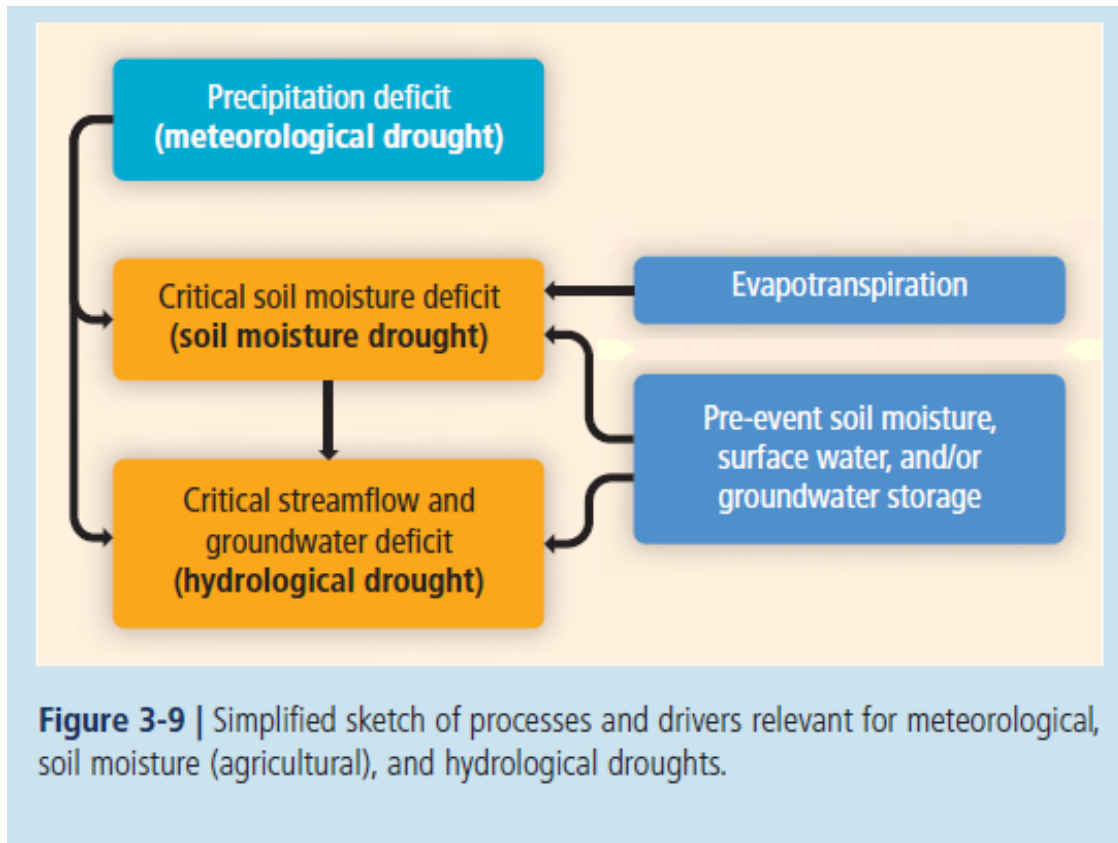
□ significant at the 99% conf. level



The following terms indicate the assessed likelihood:

Term*	Likelihood of the Outcome
<i>Virtually certain</i>	99–100% probability
<i>Very likely</i>	90–100% probability
<i>Likely</i>	66–100% probability
<i>About as likely as not</i>	33–66% probability
<i>Unlikely</i>	0–33% probability
<i>Very unlikely</i>	0–10% probability
<i>Exceptionally unlikely</i>	0–1% probability

* Additional terms that were used in limited circumstances in the Fourth Assessment Report (*extremely likely*: 95–100% probability, *more likely than not*: >50–100% probability, and *extremely unlikely*: 0–5% probability) may also be used when appropriate.



IPCC AR5 – WGII Chapter 23, First Order Draft, September 2012

IPCC SREX Report, 2012

Drought Indices

Because of the complex definition of droughts, and the lack of soil moisture observations (Section 3.2.1), several indices have been developed to characterize (meteorological, soil moisture, and hydrological) drought (see, e.g., Heim Jr., 2002; Dai, 2011). These indicators include land surface, hydrological, or climate model simulations (providing estimates of, e.g., soil moisture or runoff) and indices based on measured meteorological or hydrological variables. We provide here a brief overview of the wide range of drought indices used in the literature for the analysis of recent and projected changes. Note that information on paleoclimate proxies such as tree rings, speleothems, lake sediments, or historical evidence (e.g., harvest dates) is not detailed here.

Drought Indices

SPI – Standard Precipitation Index

CDD – Consecutive Dry Days

SMA – Soil Moisture Anomalies

PDSI – Palmer Drought Severity Index

PPEA – Precipitation Potential Evaporation Anomaly

- WGI – **OBSERVATIONS**
Second Order Draft, September 2012

There is *low confidence* in observed large-scale trends in drought, due to lack of direct observations, dependencies of inferred trends on the index choice, and geographical inconsistencies in the trends (see Table SPM.1). {2.6.2}

R5 – WGI Chapter 23, First Order Draft, September 2012
PROJECTIONS

There is *medium confidence* that droughts will intensify in the 21st century in some seasons and areas, due to reduced precipitation and/or increased evapotranspiration. This applies to regions including southern Europe and the Mediterranean region, central Europe, central North America, Central America and Mexico, northeast Brazil, and southern Africa. Elsewhere there is overall *low confidence* because of inconsistent projections of drought changes (dependent both on model and dryness index). Definitional issues, lack of observational data, and the inability of models to include all the factors that influence droughts preclude stronger confidence than *medium* in drought projections. See Figure SPM.5. [3.5.1, Table 3-3, Box 3-3]

IPCC AR5-WG1 – Second Order Draft, September 2012

Projected global CDD and SMA

Figure 3-10 | Projected annual and seasonal changes in dryness assessed from two indices for 2081-2100 (bottom three rows, showing the annual time scale and two seasons, DJF and JJA) and 2046-2065 (top, annual time scale) with respect to 1980-1999. Left column: changes in the maximum number of CDD (days with precipitation <1 mm), based on 17 GCMs contributing to the CMIP3. Right column: changes in soil moisture (soil moisture anomalies, SMA), based on 15 GCMs contributing to the CMIP3. Increased dryness is indicated with warm colors (positive changes in CDD and negative SMA values). The maps show differences between the annual and seasonal averages over the respective 20-year periods, that is, the average of 2081-2100 or 2046-2065, respectively (based on simulations under emission scenario SRES A2), minus the average of 1980-1999 (from corresponding simulations for the 20th century). Differences are expressed in units of standard deviations, derived from detrended per year annual or seasonal estimates, respectively, from the three 20-year periods 1980-1999, 2046-2065, and 2081-2100 pooled together. Color shading is only applied for areas where at least 66% of the GCMs (12 out of 17 for CDD, 10 out of 15 for soil moisture) agree on the sign of the change; stippling is applied for regions where at least 90% of the GCMs (16 out of 17 for CDD, 14 out of 15 for soil moisture) agree on the sign of the change. Adapted from Orłowsky and Seneviratne (2011); updating Tebaldi et al. (2006) for SMA and for additional CMIP3 models, and including seasonal time frames. For more details, see Appendix 3.A.

EUROPE – Changes in the length of dry spells

Figure 23-4: Projected changes in the 95th percentile of the length of dry spells for the period 2071-2100 compared to 1971-2000 (in days). Dry spells are defined as periods of at least 5 consecutive days with daily precipitation below 1mm. Changes represent average over 20 regional model simulations taken from EU-ENSEMBLES project. Hatched areas indicate regions with robust (at least 66% of models agree in the sign of change) and/or statistical significant change (significant on a 95% confidence level using Mann-Whitney-U test). For the eastern part of Turkey, unfortunately no regional climate model projections are available. Based on CMIP3 data, will be substituted by CMIP5 CORDEX data.

IPCC AR5 – WGII Chapter 23, First Order Draft, September 2012

EUROPE – Changes in the number of heat waves

Figure 23-2: Projected changes in the mean number of heat waves occurring in the months May to September for the period 2071-2100 compared to 1971-2000 (number per season). Heat waves are defined as periods of at least 5 consecutive days with daily maximum temperature exceeding the normal daily maximum temperature of the May to September season of the control period (1971-2000) by at least 5°C. Changes represent average over 9 regional model simulations taken from the EU-ENSEMBLES project. Hatched areas indicate regions with robust (at least 66% of models agree in the sign of change) and/or statistical significant change (significant on a 95% confidence level using Mann-Whitney-U test). For the eastern part of Turkey, unfortunately no regional climate model projections are available. Based on CMIP3 data, will be substituted by CMIP5 CORDEX data.

Droughts in Europe

Lack of observational data and the complex definition of droughts make the analyses of observed changes in drought characteristics difficult (SREX, Chapter 3, Box 3-3). Southern Europe has experienced trends toward more intense and longer droughts, but there are still inconsistent. Drought trends in all other subregions were not statistically significant (SREX chapter 3, section 3.5.1). Regional and global climate simulations project (with medium confidence) an increase in duration and intensity of droughts in central and southern Europe and the Mediterranean region using different definitions of droughts (SREX chapter 3, section 3.5.1). Figure 23-4 illustrates projected changes the length of dry spells for the period 2071-2100 compared to 1971-2000 (in days). The projected increase in dry spells is much greater in Southern Europe.

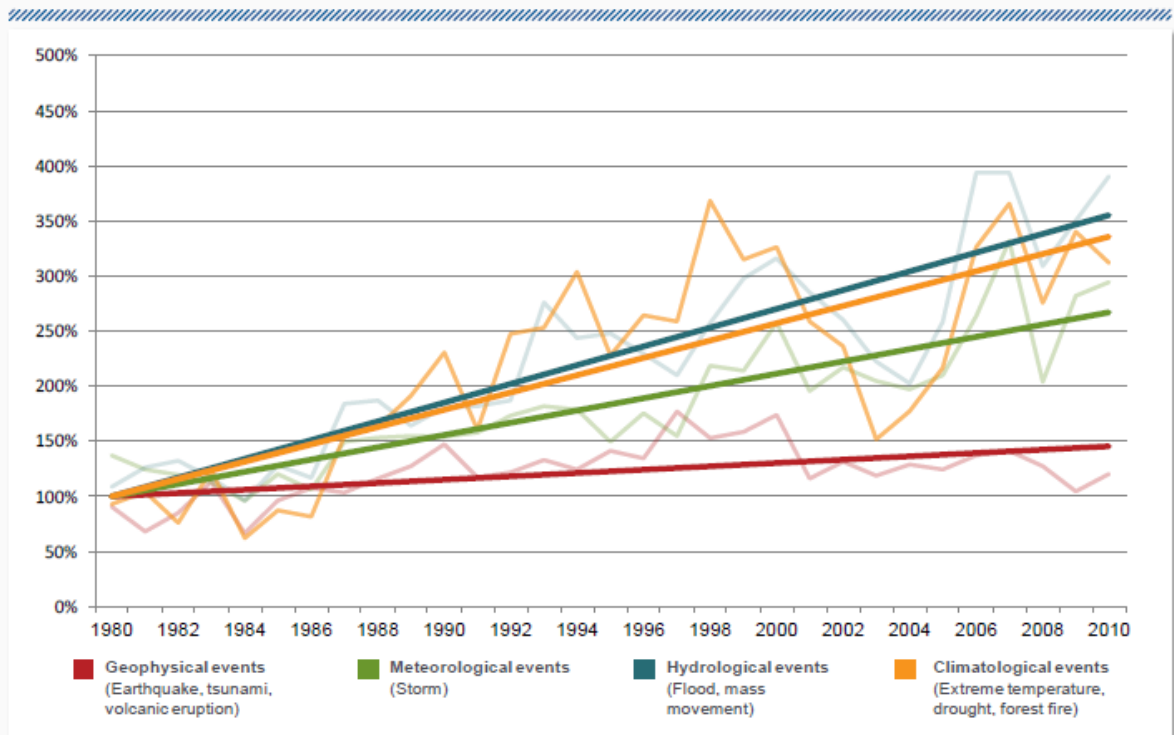
IPCC AR5 WGII – Chapter 23 - First Order Draft, September 2012

Economic Impacts of Extreme Weather Events

Much of the information we have about the economic impacts of extreme weather events comes from data on insured losses compiled by insurance industry. In the preparation of this report we have benefited from analysis of a particular data set, held by the Munich Re company in its NatCat Service, comprising about 30,000 data sets of individual loss events caused by natural hazards. This analysis shows that in general, the frequency of weather-related loss events has increased significantly at a global level, in contrast with losses from geophysical hazards such as earthquakes or tsunamis, which have shown only a slight increase.

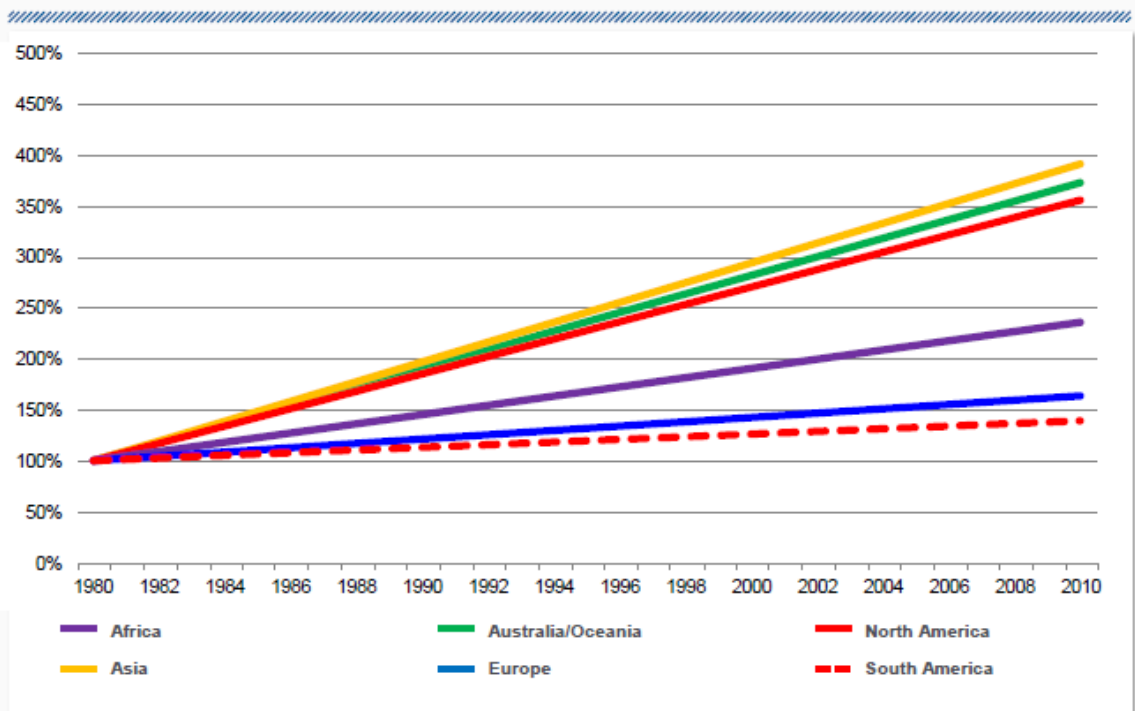
Natural catastrophes worldwide 1980 – 2010

Number of events with relative trends

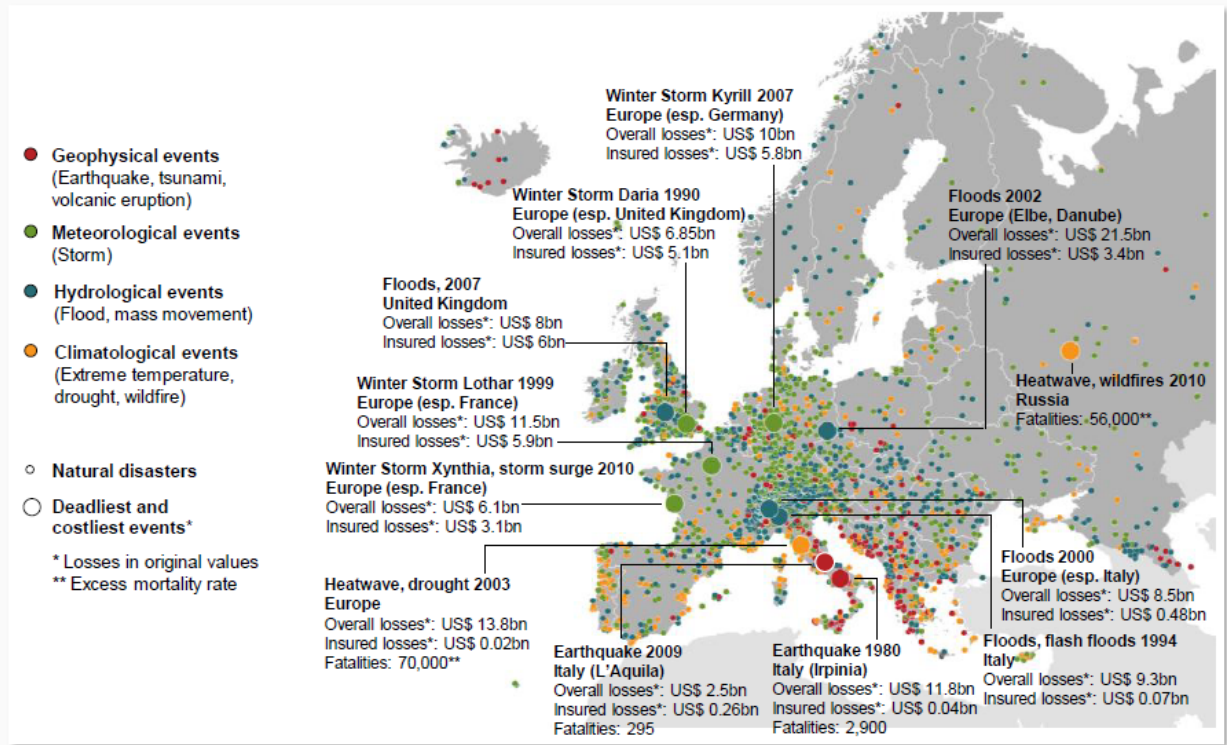


Natural catastrophes worldwide 1980 – 2010

Number of events – relative trends by continent

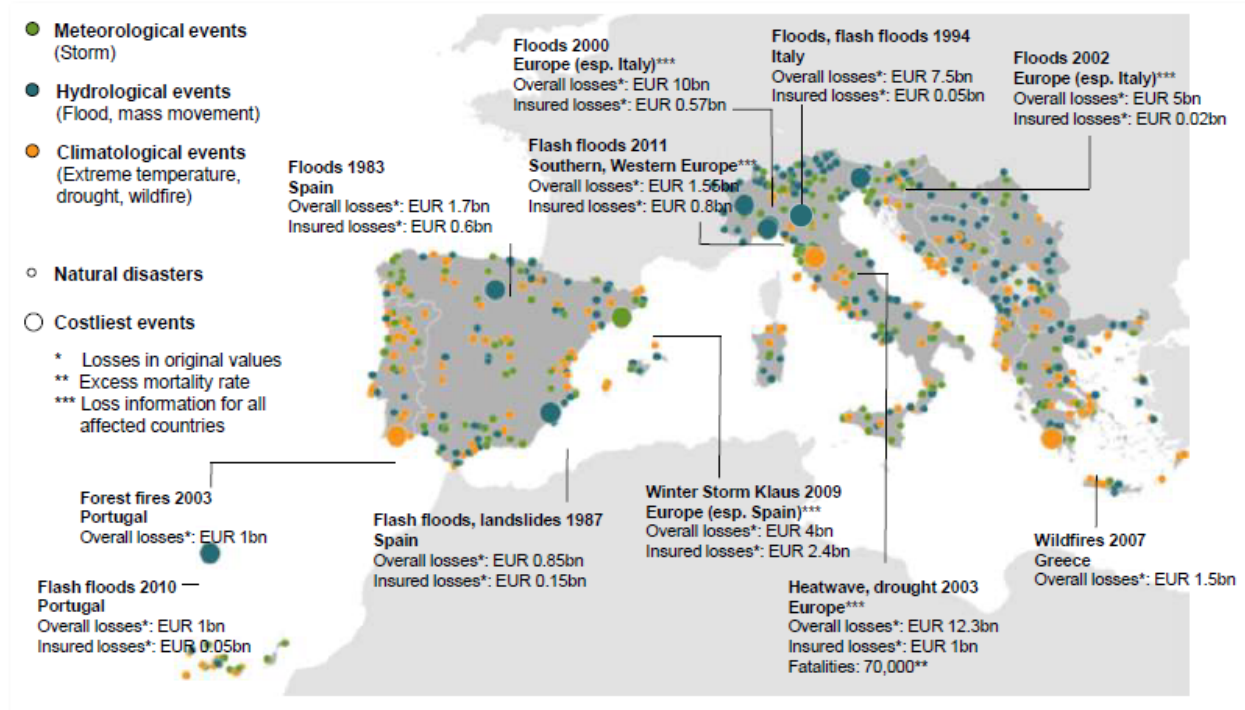


Map



Weather Catastrophes in Southern Europe 1980 – 2011

Map



In Europe the increase in loss events from extreme weather events has been about 70% since the 1980s. This is low compared with the number of loss events suffered in other continents which in the case of North America are now 3.7 times the numbers of the early 1980s. Of these loss events registered in the NatCatService database, the great majority (91%) are from extreme weather and of these most (75%) are from storms and floods..

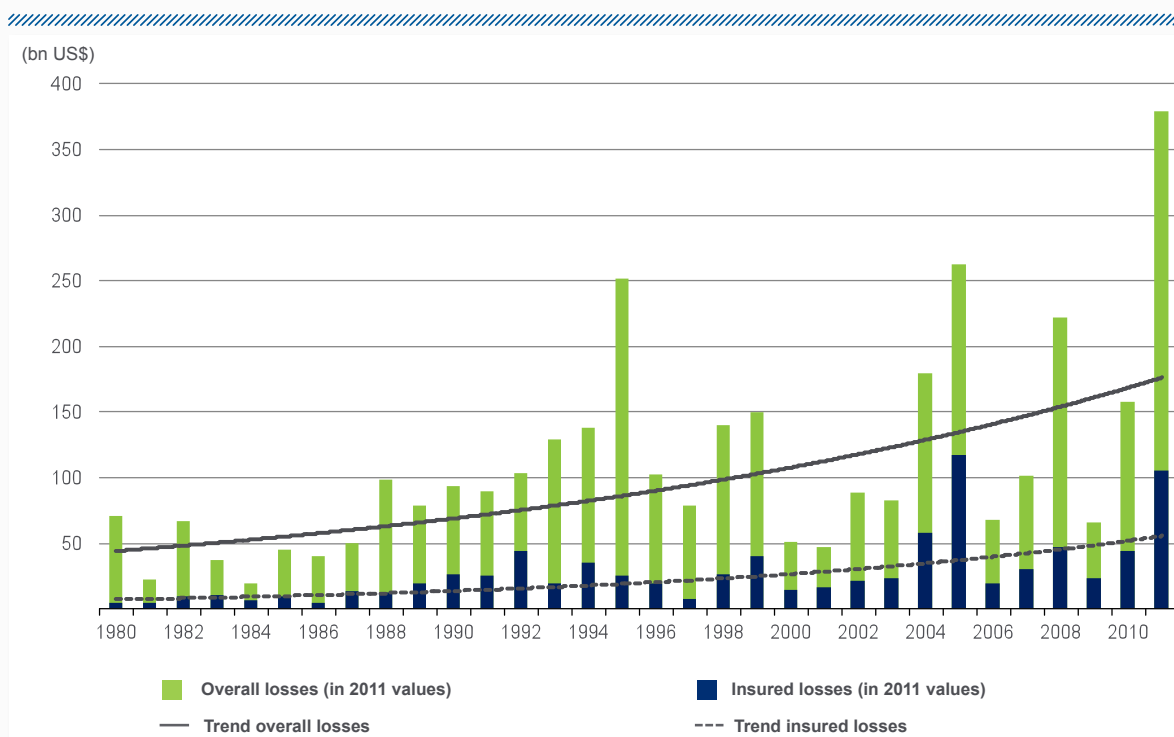
The pattern of loss events varies across Europe, with larger numbers in the UK and West-Central Europe and lower numbers in Scandinavia and Northern Europe. In Southern Europe, heatwaves, droughts and wild-fires are the most numerous events, in Western and Central Europe floods and storms predominate.

NatCatSERVICE

Natural catastrophes worldwide 1980 – 2011

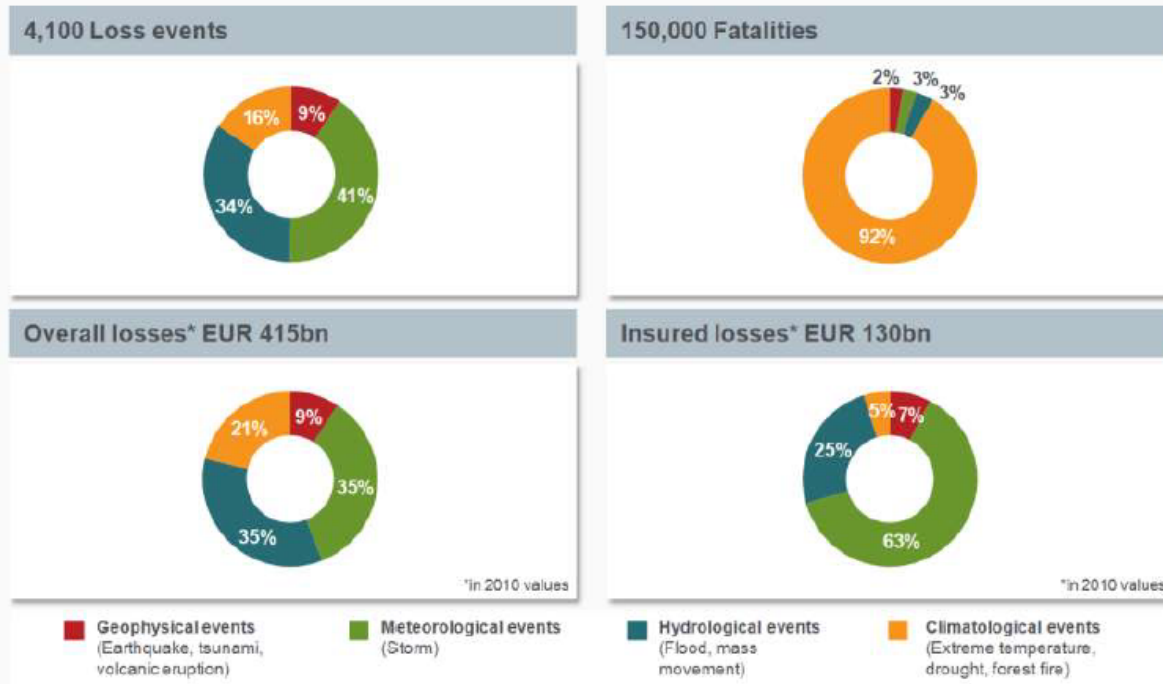
Munich RE 

Overall and insured losses with trend



Natural catastrophes in Europe 1980 – 2010

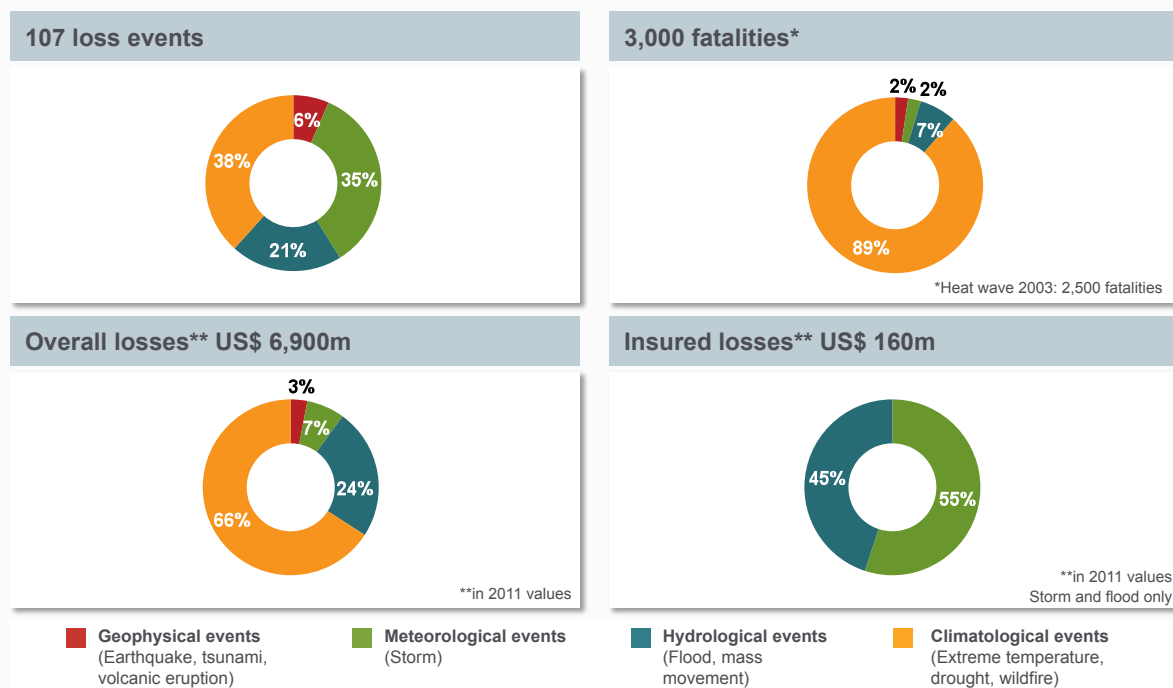
Percentage distribution



© 2011 Münchener Rückversicherungs-Gesellschaft, Geo Risks Research, NatCatSERVICE – As at January 2011

Natural catastrophes in Portugal 1980 – 2011

Percentage distribution



© 2012 Münchener Rückversicherungs-Gesellschaft, Geo Risks Research, NatCatSERVICE – As at April 2012

The economic loss burden has been considerable, with an estimated loss of Euros 460 billion since 2008 (2011 values). The most costly hazards have been storms and floods, amounting to a combined total of over Euros 300 billion.

Weather events have also been responsible for considerable loss of life in Europe, estimated at around 140,000 lives lost since 1980. The largest impacts on life have come from heatwaves such as those of central Europe in 2003.

Climate change will increase the frequency and intensity of heat waves, particularly in Southern Europe [high confidence, high agreement] with adverse implications for health, agriculture, energy production, transport, tourism and housing.

Heat-related mortality and morbidity will increase [medium confidence], particularly in Southern Europe.

Climate change may change the distribution and seasonal activity of some human infections, including those transmitted by arthropods [medium confidence, low evidence].

IPCC WGII

Conclusões

- Em média irá chover entre menos 28% (A2) e 19% (B2) no final do século
- As temperaturas máxima e mínima irão aumentar entre 3°C (A2) e 2°C (B2) no final do século
- Extremos de calor irão aumentar no final do século e os extremos de frio diminuir
- Nos meses de Maio, Junho e Outubro haverá um maior aumento da temperatura máxima e mínima
- Nestes meses a temperatura máxima irá aumentar mais de 4°C no final do século para o cenário A2
- Para a temperatura mínima o aumento é mais homogêneo ao nível dos meses, mas haverá um aumento ligeiramente maior nos meses de Fevereiro, Maio e Junho

Conclusões

- Em geral haverá um aumento da precipitação nos meses de Março, Julho e Agosto e uma diminuição nos restantes meses no final do século
- O aumento da precipitação no Verão será maior no litoral do que no interior
- No Inverno o aumento da temperatura máxima será ligeiramente inferior no interior
- No Verão o aumento da temperatura máxima irá ser menor no interior, com excepção das terra altas e no interior sul da área de estudo
- O aumento da temperatura mínima no Inverno será maior na zona central da área de estudo com tendência para o litoral
- No Verão a temperatura mínima irá aumentar mais na zona interior do país, principalmente nas terra altas